Revealing the unknown world of the endangered Lear's macaw using GPS-tracking data: identification of critical habitats for conservation

FERNANDA R. PASCHOTTO[1] orcid.org/0000-0002-6651-8318, ERICA C. PACÍFICO[2] orcid.org/0000-0003-3518-1887, THIAGO FILADELFO[3] orcid.org/0000-0002-0523-9788, GABRIELA R. FAVORETTO[4] orcid.org/0000-00026382-140X, JULIA E. F. OSHIMA[5] orcid.org/0000-0003-1545-768X, PAULO CARDOSO[6] orcid.org/0000-0001-5458-998X, FRANCISCO V. DÉNES[7] orcid.org/0000-0002-9870-7682

[1]contact e-mail: fernandarpaschotto@gmail.com | Movement Ecology Lab, Department of Ecology, Institute of Biosciences, University of São Paulo. Rua do Matão, travessa 14, nº 321, Cidade Universitária, 05508-090, São Paulo/SP, Brazil
[2]ericapacifico81@gmail.com | Department of Animal Biology, Institute of Biology, State University of Campinas. Rua Monteiro Lobato, nº 255, Cidade Universitária, 13083-862, Campinas/SP, Brazil
[3]thiago_bioufba@yahoo.com.br | Rua Ana C. B. Dias, Condomínio Jardim Atlântico, Casa E8, Miragem, 42709-500, Lauro de Freitas/BA, Brazil
[4]gabifavoretto@yahoo.com.br | Av. Mario Ybarra de Almeida, nº 841, Centro, 14800-420, Araraquara/SP, Brazil
[5]juliaoshima@yahoo.com.br | Movement Ecology Lab, Department of Ecology, Institute of Biosciences, University of São Paulo. Rua do Matão, travessa 14, nº 321, Cidade Universitária, 05508-090, São Paulo/SP, Brazil
[6]paulo.c@bioinsight.pt | Bioinsight, Lda. Rua Antero de Quental, nº 52 B, Urbanização Colinas do Cruzeiro, 2675-690, Odivelas, Portugal
[7]francisco.denes@ib.usp.br | Movement Ecology Lab, Department of Ecology, Institute of Biosciences, University of São Paulo. Rua do Matão, travessa 14, nº 321, Cidade Universitária, 05508-090, São Paulo/SP, Brazil

Word count: 6,998

Article

Revealing the unknown world of the endangered Lear's macaw using GPS-tracking data: identification of critical habitats for conservation

FERNANDA R. PASCHOTTO*[1,2] orcid.org/0000-0002-6651-8318, ERICA C. PACÍFICO[2,3] orcid.org/0000-0003-3518-1887, THIAGO FILADELFO[2] orcid.org/0000-0002-0523-9788, GABRIELA R. FAVORETTO[2] orcid.org/0000-00026382-140X, JULIA E. F. OSHIMA[1] orcid.org/0000-0003-1545-768X, PAULO CARDOSO[4] orcid.org/0000-0001-5458-998X, FRANCISCO V. DÉNES[1,5] orcid.org/0000-0002-9870-7682

*Corresponding author, fernandarpaschotto@gmail.com
[1]Department of Ecology, University of São Paulo, São Paulo, Brazil
[2]Lear's Macaw Research and Conservation Group (GPCA), São Paulo, Brazil
[3]Department of Animal Biology, State University of Campinas, Campinas, Brazil
[4]BE Bioinsight | ECOA, Environmental Consultants, Portugal
[5]Department of Migration, Max Planck Institute of Animal Behavior, Konstanz, Germany

Abstract Understanding space use and home range is essential for the conservation planning of threatened species as it helps to assess the suitability, extent, and placement of conservation areas that are imperative for species survival and protection. The Endangered Lear's macaw (*Anodorhynchus leari*), a highly mobile frugivore, feeding specialist and endemic to Brazil's Caatinga dry forest, faces ongoing habitat degradation. In this study, we identified critical habitats by examining the spatial distribution of feeding, resting, and roosting sites and investigating home range size and its temporal variation. We GPS-tracked juvenile macaws and estimated fortnightly home ranges with autocorrelated kernel density estimators. We assessed if extrinsic factors, such as tagging site, seasonality, rainfall and vegetation productivity (proxies for food availability) influenced home range size. Our findings reveal considerable variation in home ranges, with an average of 850.15 km^2 (1.24-8,549.48 km^2). Home ranges expanded significantly during the dry season (mean 1,097.06 km^2), representing a 2.14-fold increase from the wet season. We also found that site and season primarily drove home range size, while vegetation productivity and rainfall had limited influence. This suggests that macaw movements may respond to complex interactions between rainfall, landscape composition and configuration, and food availability rather than direct resource fluctuations. This is the first study to estimate home ranges for Lear's macaw, providing critical insights into its spatial ecology. Our findings underscore the importance of preserving key roosting and feeding areas and highlight the need for continuous monitoring to address threats posed by environmental changes and human activity.

Keywords Caatinga, conservation, GPS tracking, habitat use, home range, Lear's macaw, licuri palm, parrot

The supplementary material and code on GitHub for the analysis in R for this article are available at https://doi.org/xxx

Introduction

Understanding space use and home range is essential for wildlife conservation, providing insights into movement patterns, species' distribution, ecological needs, and spatial requirements (Adamek, 2011; Walton et al., 2017). Habitat loss is one of the main drivers of species extinction, especially for endemic and/or specialist species (Morato et al., 2018; Oliveira et al., 2021), and this knowledge can help identify suitable environments for threatened species and guide conservation actions, such as protecting feeding and breeding sites across their distribution ranges, many of which remain poorly understood, and providing quantitative information that may help delineate adequate protected areas, evaluating their distribution and extent as needed for the maintenance of these species (Schofield et al., 2010; Goldingay, 2015; Yeap et al., 2021).

The Lear's macaw (*Anodorhynchus leari*), an Endangered frugivore endemic to the Caatinga dry forest in northeastern Brazil, exemplifies the challenges of conserving species with highly specialized habitat requirements (BirdLife International, 2020). The macaw's survival is closely tied to the availability of licuri palm (*Syagrus coronata*) fruits, and it nests and roosts primarily on sandstone cliffs (Pacífico et al., 2014). However, recent observations indicate that some individuals also roost in trees, though the ecological significance of this behaviour is not fully understood (E.C.P. pers. comm., 2023).

Despite its restricted range, significant knowledge gaps persist regarding the species' movement patterns, seasonal variation in space use, and the drivers of home range size. Habitat degradation, compounded by desertification and anthropogenic activities, threatens key feeding and roosting sites (Santos Neto & Camandaroba, 2008; Barbosa & Tella, 2019). Tracking macaws' movements in their often-inaccessible natural habitat is challenging, limiting our understanding of their spatial ecology and our ability to identify and protect critical habitat for the species (Le Souef et al., 2013; Yeap et al., 2017; Brightsmith et al., 2021).

To address these gaps, we investigated Lear's macaw space use by examining home range size, seasonal variation, and the spatial distribution of feeding, resting, and roosting sites. Specifically, we formulated the following research questions: (1) Where are the feeding, roosting and diurnal resting sites? (2) How is the habitat of these sites characterized? (3) How extensive are individual home ranges? (4) Do these ranges and movement patterns vary seasonally?

By combining Global Positioning System (GPS) tracking data with remote sensing and environmental variables, we aim to provide critical information to inform conservation efforts for this emblematic species of the Caatinga.

Study area

The study region encompasses the distribution of Lear's macaw in northern Bahia, Brazil, within the Caatinga Phytogeographical Domain (Fig. 1; Moro et al., 2016; BirdLife International, 2020). The eastern range includes the nine known roosting sites (sandstone cliffs and trees) in *Raso da Catarina* region, concentrating the main population of macaws, with the protected areas *Estação Biológica de Canudos* and *Estação Ecológica do Raso da Catarina*. The western range, known as *Boqueirão da Onça* and located 230 km west, includes the recently established protected areas *Área de Proteção Ambiental* and *Parque Nacional Boqueirão da Onça*. This range holds another currently disjunct population that declined sharply in the last decades. By 2019, it was functionally extinct with only two non-breeding adult macaws. Since that year, a long-term reintroduction and monitoring program has been releasing rescued, confiscated and captive-bred macaws (GPCA, 2024).

The Caatinga is one of the largest tropical semi-arid areas in the world (Moro et al., 2016), where the seasonally tropical dry forests prevail as dominant vegetation, consisting of a mosaic of different physiognomies spanning a broad range of woody plant densities and shrubs. The climate is semiarid, and the average mean temperature is constant and high over the year, ranging 25-30ºC. The region presents a wide spatiotemporal variation in annual and interannual rainfall, with most of the territory (68.8%) receiving 600-1,000 mm of annual precipitation, and 20% receiving less than 600 mm. However, this rainfall is concentrated over a few months of the year (Silva et al., 2017). Thus, the vegetation is under seasonal hydric deficiency, experiencing long drought periods. Regionally, vegetation dynamics vary widely across time and space and are strongly correlated with rainfall. Most plants usually lose their leaves in the dry period and grow and produce flowers and fruits during the short-wet season (Silva et al., 2017; Fernandes et al., 2020).

The combination of acute human disturbances (e.g., conversion of large areas of native vegetation into roads, energy infrastructure, or commercial agriculture), chronic disturbances (e.g., slow but continuous native vegetation overexploitation, slash-and-burn agriculture, and browsing by livestock), proliferation of exotic species (e.g., Africanized honey bees; Pacífico et al., 2020) and climate change can lead to severe degradation of natural habitats and disruption of critical ecological services (Silva et al., 2017). Thus, macaws face the impacts of several anthropogenic activities in their habitat, and food availability is a concern for population growth and persistence (Barbosa & Tella, 2019).

Methods

Data collection

Macaw capture, bio-logger deployment and GPS data collection

We used bio-loggers (tags) to track macaw movements. Juvenile birds were fitted with 15 g solar-powered tags (e-obs, Germany) equipped with Ultra High Frequency (UHF), GPS, and tri-axial accelerometry sensors, and attached using a Teflon ribbon harness in backpack-configuration. The total weight of the tag plus harness was about 2.4% of the mean adult body mass (720 g), following established tag weight-limit guidelines (Yeap et al., 2021). After tag deployment, we carried out monthly surveys of known roosting and feeding sites to search and monitor the tagged macaws, allowing GPS data retrieval via UHF data transmission. Before data analysis, the movement data was uploaded to and stored in Movebank (Kays et al., 2022). See Supplementary Material 1 for details on tag deployments and GPS data collection.

Data analysis

Identification of feeding, resting and roosting sites and spatial distribution of the locations

We identified the main feeding, resting and roosting sites using the "Roost and Foraging Site Extraction" MoveApps workflow (Kölzsch et al., 2023), by extracting mean coordinates of daily diurnal and nocturnal locations of high GPS fix density where macaws stayed in a defined radius for a defined minimum duration, not moving faster than 1 m/s (GPS ground speed). Before the identification of these sites, all GPS fixes were classified as day or night positions, delineated by sunrise + 30 min and by sunset - 60 min (as macaws tend to leave roosting sites about 30 min after sunrise, and stay at foraging sites until about 60 min before sunset; E.C.P. field observation, 2008).

Feeding sites were defined as all sites at daylight where a macaw stayed for at least 5 h within a radius of 1,000 m. The resting sites were defined as all sites during daytime where a macaw stayed for at least 3 h (minimum resting duration) within a radius of 50 m. Lastly, the roosting sites were defined as all sites during nighttime where a macaw stayed for at least 9 h within a radius of 500 m. Radii and time intervals selected to identify feeding, resting and roosting sites were established considering the species' daily movements between roosting areas and feeding sites, and observed behaviour; the 9-hour minimum interval at night was defined based on the known roosting behaviour, and to be long enough to fully include the tag battery-saving sleep mode (7pm – 4am). See Supplementary Material 2 for details on the MoveApps analysis protocol.

To spatially characterize the identified locations, we calculated the distances between the resting sites to the closest feeding sites, and the distances between the resting and feeding sites to the closest roosting sites using the "Distance Matrix" tool in QGIS (QGIS Development Team, 2023).

Habitat characterization

We characterized the environments visited by the macaws with variables representing anthropogenic features, land cover and topography. We derived rasters with the calculated Euclidean distances from both the medium-voltage power lines (ANEEL, 2024) and roads (DNIT, 2021) networks. We used land cover and land use rasters from MapBiomas to characterize the landscape composition with natural vegetation and anthropogenic activities (Franca Rocha et al., 2024; MapBiomas, 2024). With the same purpose, we used the Human Modification Degree index (Kennedy et al., 2019), a continuous metric varying from 0-1 that reflects the proportion of a landscape that is modified based on modelling physical extents of 13 main anthropogenic stressors (with global coverage) and their estimated impacts. Finally, we also derived mean slope values (degrees) from Copernicus Global Digital Elevation Model (European Space Agency, 2024). The locations previously identified were then overlapped onto GIS remote sensing layers obtained. See Supplementary Table 1 for more detailed information.

Movement data processing and generation of subsets prior to home range estimation

To account for potential location errors before estimating individual home ranges, the user equivalent range error (UERE) was calculated using the ctmm package in R (Calabrese et al., 2016; Fleming et al., 2020). GPS points were collected while tags remained stationary for 10-14 hours in the study area to estimate the UERE values. The horizontal UERE of 0.437 m (95% CI: 0.377-0.497) was incorporated into the dataset.

Following this calibration, individual tracking data were divided into 15-day intervals (fortnightly subsets) using R (R Core Team, 2023), resulting in 211 subsets spanning May 2017 to May 2023 (Supplementary Table 2). These intervals allowed the assessment of temporal variation in range sizes. Using the fortnightly subsets, we generated 211 home range and core area estimates, as detailed in supporting materials (Supplementary Table 3).

Home range and core area estimation, and environmental effects

We estimated fortnightly individual home ranges and core areas (Supplementary Table 3) with GPS data using autocorrelated kernel density estimators (AKDE) with the ctmm R package (R Core Team, 2023). The home ranges were calculated using 95% AKDE, corresponding to the individual's mobility potential; and the core areas, using 50% AKDE, corresponding to the areas the animal uses most frequently (Fleming et al., 2015; Calabrese et al., 2016). Calculating macaws' ranges every 15 days allowed us to assess changes in home range and core area size throughout the annual cycle and compare their variation size between seasons. See Supplementary Material 3 for more details on home range and core area estimation method.

Estimated ranges of birds with more than one year of movement data (Supplementary Table 4; IDs 5568, 5570, 6444, 9025) were evaluated concerning interannual and seasonal variation. The selection of predictor variables was based on their expected influence on the macaws' movement. Using a linear model (bbmle R package; Rencher & Schaalje, 2008), we explored if extrinsic factors were good predictors of home range and core area size. We evaluated the effect of site (i.e., roosting site where each macaw was born – or released – and tagged, and from where the individual performs daily movements to forage), season ("wet" versus "dry"), ordinal date, rainfall precipitation and vegetation productivity (both proxies of licuri palm fruit availability; see Supplementary Material 4 for details on environmental predictors and data processing, and Supplementary Table 5 for rainfall and Normalized Difference Vegetation Index (NDVI) data).

Home range and core area size model

We tested models that considered the influence of one variable (i.e., the variables were analysed independently), and models that considered the influence of two variables (pairwise), with and without interaction (Supplementary Tables 6 and 7 for home range and core area analysis, respectively). Pearson's correlation coefficients (r) were calculated (Supplementary Table 8), and the predictor variables with $|r| > 0.6$ were excluded from combined models. For the pairwise analysis, different variables selected to represent the seasonal variation (i.e., season, ordinal date, accumulated rainfall and NDVI data) were not evaluated together in the same model. Also, the variables “tagging site” and “year of monitoring” were not evaluated simultaneously in the same model due to correlation, because for a specific monitoring time frame, movement data was only available for individuals born in the same breeding site. In those cases, the variable “tagging site” was tested in the models.

We used the AIC to rank models and selected the model with the lowest value (Akaike, 1987; Burnham & Anderson, 2002). Moreover, we calculated the adjusted coefficient of determination (R^2) as a measure of how much of the observed variation was explained by the linear relationship with the explanatory variables included in the model (Su et al., 2012; bbmle and AICcmodavg R packages; R Core Team, 2023).

Results

We collected GPS data from 2017 to 2024 (Supplementary Table 4). Although we retrieved movement data from 11 juvenile macaws tracked during this period, some individuals had limited tracking periods (< 45 days, or < 10 days of data; Supplementary Table 4). Data from these individuals represented 1% of the total GPS fixes of the telemetry dataset. While this data was included in the descriptive analysis and environmental characterizations, it was excluded from subsequent home range analyses. The tracking duration for individual macaws ranged from four to 1,346 days, and the average tracking period was 347 days (SD = 486.12). The final dataset consisted of 841,761 GPS fixes, spanning seven years (2017 – 2024; except the year 2020, for which no movement data was retrieved). The number of GPS fixes per individual ranged from 178 to 668,473 (Supplementary Table 4), with mean and median values of 76,524 and 2,356 points, respectively.

Identification of feeding, resting and roosting sites and spatial distribution of the locations

We identified 3,038 feeding, 1,228 resting and 2,923 roosting locations, distributed in *Boqueirão da Onça* (Fig. 1d,f) and *Raso da Catarina* regions (Fig. 1h,j).

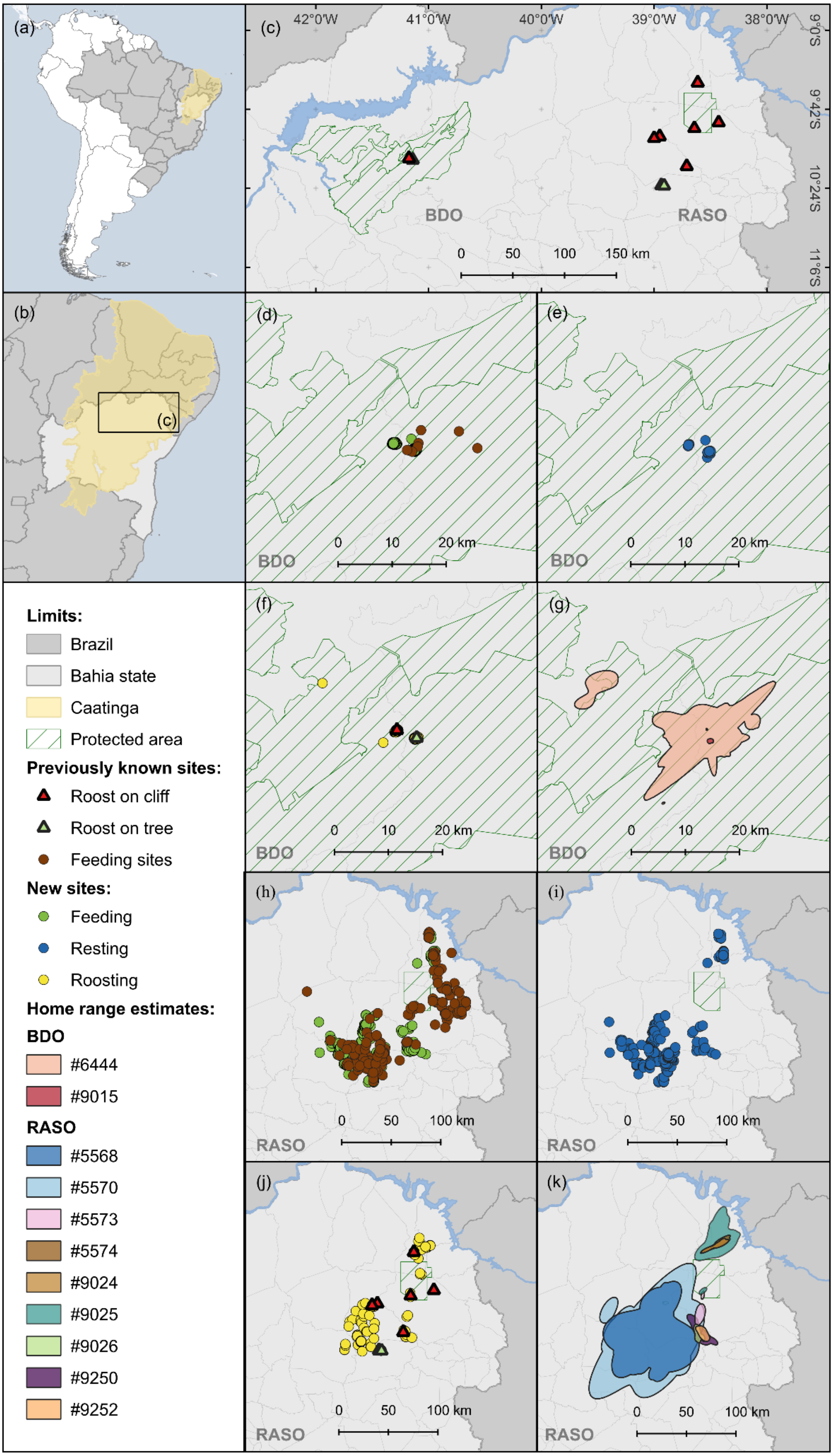
(a)
(b)
(c)
42°0'W
41°0'W
40°0'W
39°0'W
38°0'W
9°0'S
9°42'S
10°24'S
11°6'S
BDO
RASO
0
50
100
150 km
(d)
(e)
(f)
(g)
(h)
(i)
(j)
(k)
0
10
20 km
0
50
100 km
Limits:
Brazil
Bahia state
Caatinga
Protected area
Previously known sites:
Roost on cliff
Roost on tree
Feeding sites
New sites:
Feeding
Resting
Roosting
Home range estimates:
BDO
#6444
#9015
RASO
#5568
#5570
#5573
#5574
#9024
#9025
#9026
#9250
#9252

FIG. 1 (a) Caatinga Domain in northeastern Brazil. (b) Study area in northern Bahia state, comprising the (c) *Boqueirão da Onça* (BDO; left) and *Raso da Catarina* (RASO; right). (d-f) Feeding, resting, roosting sites and (g) total home ranges of two macaws tagged in BDO; (h-j) Feeding, resting, roosting sites and (k) total home ranges of nine macaws tagged in RASO. Total home ranges were estimated by combining all the fortnightly individual ranges using the "Merge" tool in QGIS software (QGIS Development Team, 2023). Previous feeding areas database: GPCA data collected over the last 10 years, CEMAVE and Silva-Neto et al. (2012).

The resting sites were located very close to the feeding areas, with a median distance of only 19.8 meters to the nearest feeding site (Supplementary Table 9). Additionally, there were records of resting areas (2.5%) overlapping feeding locations (minimum distance = 0). The median distance to the nearest roosting site was 361.52 m; the feeding sites, in turn, were closer to the roosting sites (median distance = 201.13 m; Supplementary Table 9). Both feeding and resting sites were located as far as 36 km from the nearest roost.

Spatiotemporal analysis

Macaws spent about 8 hours daily (median, ranging 5-11 h duration) in foraging sites, within a median radius of 431 meters (Supplementary Table 10). In comparison, the time spent in resting sites was almost two times shorter, with a median value of 4.2 h (ranging 3-10.5 h during the day), and a median radius of only 18.2 m. The night data, in turn, indicated that macaws roosted about 12 h per night (ranging 9-14 h; Supplementary Table 10), within a median radius of 160 m.

The feeding behaviour started early in the day, with macaws leaving roosts and initiating exploration of the foraging sites around 05:30-06:30 am (Fig. 2a). The start times of resting behaviour, in turn, were more distributed until mid-morning (Fig. 2b). Both the feeding and resting activities occurred throughout the day, lasting until late afternoon (Fig. 2a,b). Moreover, during the winter, macaws tended to arrive later and leave both the feeding and resting sites earlier (Fig. 2a,b).

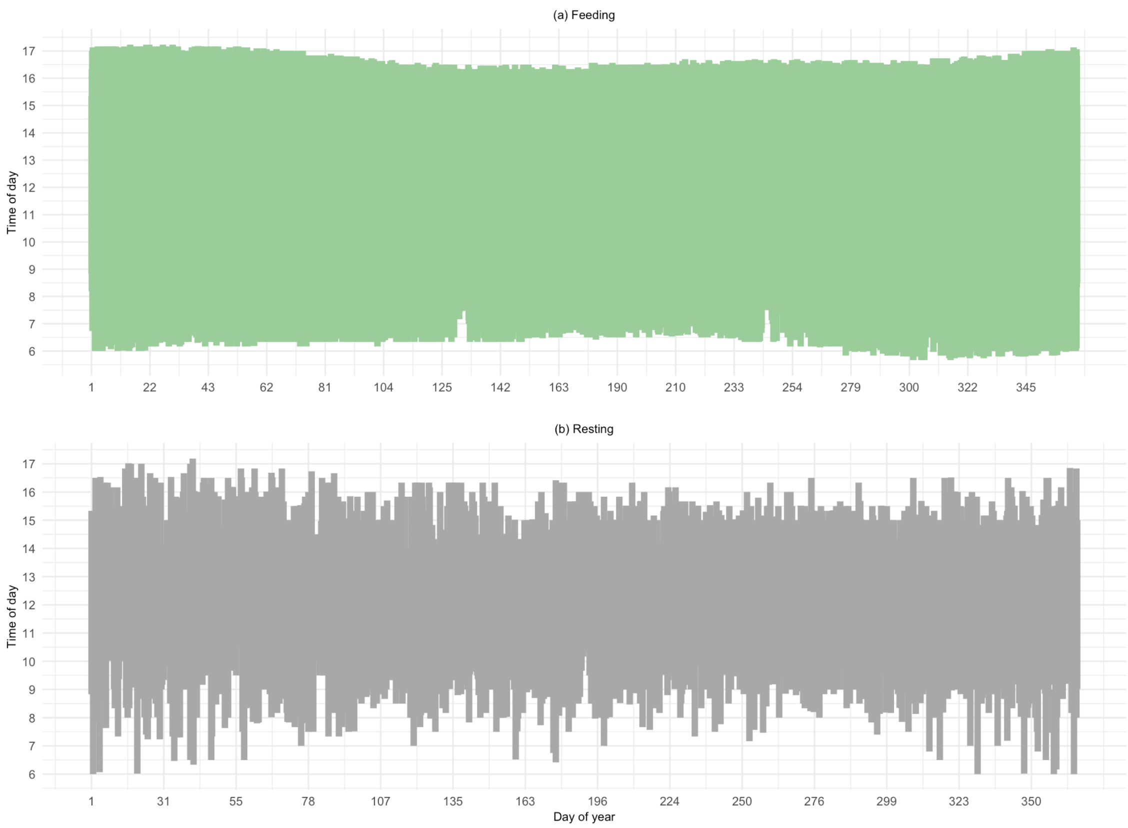

FIG. 2 Daily activity patterns, throughout the year, of macaws arriving at feeding (a) and resting (b) sites and leaving these sites to return to their roosts. Data from 2017 to 2024.

Habitat characterization

Approximately 30% of feeding and resting sites were located close to medium-voltage power lines (zero up to 1,000 m distance), while only about 10% of roosting sites were within the same range. 42% and 31% of feeding and resting sites, respectively, were also located within 10,000-12,000 m of electrical infrastructure. The feeding and resting sites also showed similar results regarding the central tendency of distance to power lines (Fig. 3a,e). For roosting sites, the median distance from power lines was about four times greater (Fig. 3i).

The feeding and resting sites also showed similar trends regarding the closeness to roads (not surprising, given that most power lines are built along roads), with more than 40% of the locations situated at distances up to 10 km (Fig. 3b,f). Almost 40% of roosting sites were also located within this range, although the median distance from roads was superior (Fig. 3j). On the other hand, about 30-40% of all the identified feeding, resting and roosting sites were located 30-35 km away from road surfaces.

Strikingly, 100% of all lands identified had some indication of human activities (HMc > 0). Once more, the feeding and resting sites presented similar results (Fig. 3c,g), with about half of their locations showing a moderate degree ($0.10 < \text{HMc} \leq 0.40$) of human modification. Although the roosting sites showed a central tendency to be in lands with a lower degree of human modification ($\text{HMc} \leq 0.1$; Fig. 3k), 35% of these sites were categorized as moderate modification ($0.10 < \text{HMc} \leq 0.40$; the maximum degree value obtained was 0.31).

The median slope, although twice as high for roosting sites, showed low values (under 6 degrees) for all identified locations (Fig. 3d,h,l), indicating that macaws also used gentler slope surfaces as roosting areas. The feeding and resting sites had a very similar distribution of values, with a higher concentration of data at lower values (Fig. 3d,h). The slope of the terrain in roosting areas (Fig. 3l), on the other hand, showed greater variation, with a higher frequency of steeper slopes, compared to feeding and resting sites. Moreover, all higher measurements (above 40 degrees) identified were located neighbouring the previously mapped sandstone cliffs used as roosts, suggesting that macaws use gentler surfaces during daylight activities.

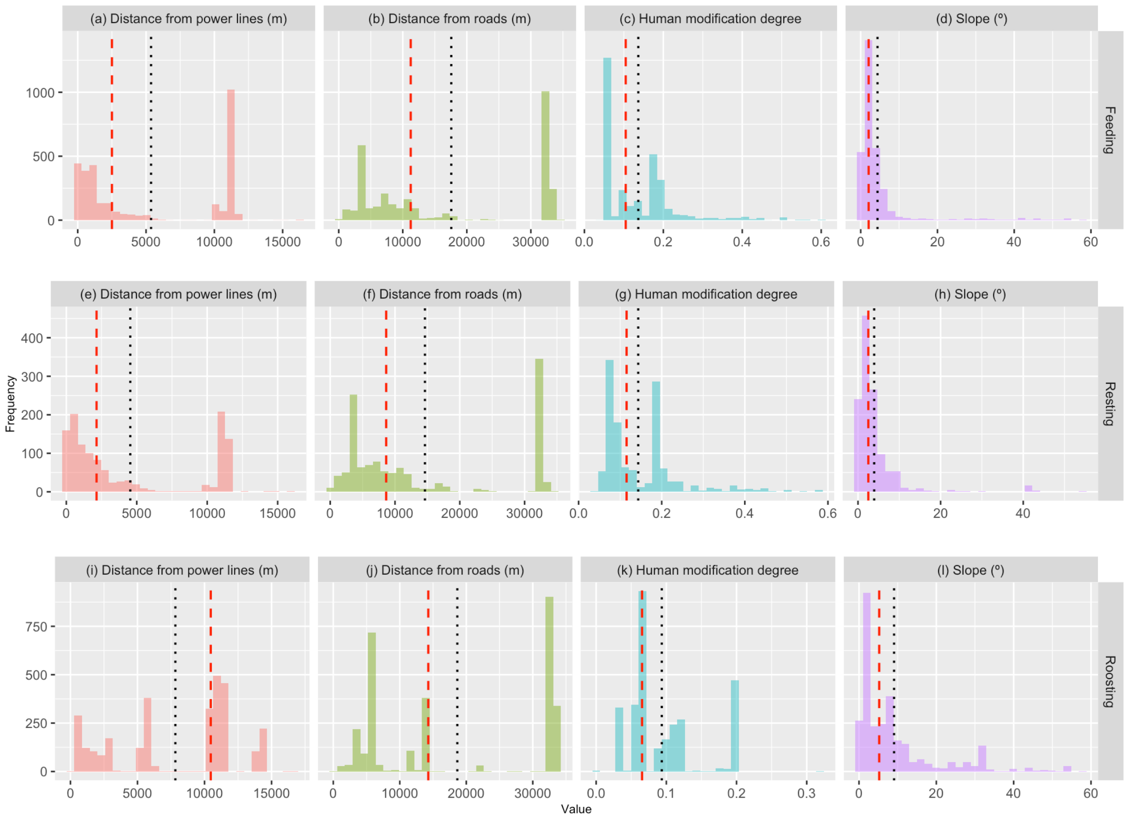

FIG. 3 Habitat characterization of feeding (a-d), resting (e-h) and roosting (i-l) locations using the continuous variables selected to represent anthropogenic features and topography. The median of each value is indicated by a red dashed line, the mean, by a black dotted line. Note the variable scale of the y-axis.

More than half of feeding and resting sites were concentrated within areas directly related to agricultural activity (Pasture and Mosaic of Uses; the latter characterized as areas where it was not possible to distinguish between pasture and agriculture), with about 50% located in non-natural Pasture lands (Fig. 4a,b). Native formations accounted for ~25% of feeding and resting sites (Forest and Savanna). On the other hand, roosting sites showed the opposite tendency, with the native vegetation cover classes accounting for 50% of locations, while 25% of locations were within agricultural use lands (Fig. 4c). It should be noted that about 20-25% of the feeding, resting and roosting sites were in Other non-Vegetated Areas (Fig. 4a-c), characterized by non-permeable surfaces, such as infrastructure, urban expansion or mining (these are clearly human-modified areas, although these surfaces could not be mapped into their specific land use classes).

FIG. 4 Habitat characterization of (a) feeding, (b) resting and (c) roosting locations using the land cover and land use variable. Note the variable scale of the y-axis.

Home range and core area estimation

All the movement models selected for the fortnightly subsets identified the residence behaviour of macaws (OU anisotropic, OUF and OUF anisotropic, and IID anisotropic (Calabrese et al., 2016); even for those individuals with less than 30 days of data; supporting information in Supplementary Table 2).

The size of fortnightly ranges of juvenile birds showed intra and interannual variation; also, the estimates varied across individuals (Fig. 5 and 6). The fortnightly analysis of overall range size indicated an average home range (95% kernel contour) of 850.2 km^2 (1.2-8,549.5 km^2; SD = 1,292.3 km^2), and an average core area (50% kernel contour) size of 198.6 km^2 (1.1-2,132 km^2; SD = 322.7 km^2); with greater variability in the size of core areas ($CV_{home\ range}$ = 1.52; $CV_{core\ area}$ = 1.625). Supporting information in Supplementary Table 3.

Macaws' dry season (June – December) ranges were highly variable, averaging 1,097.1 km^2 for the home ranges (1.7-8,549.5 km^2; SD = 1,529.8 km^2), while the core area size averaged 265.4 km^2 (1.7-2,132 km^2; SD = 387.4 km^2). The wet season (January – May) range analysis indicated the average of home ranges was 511.6786 km^2 (1.2-3,346.1 km^2; SD = 753.1 km^2), and the average of core areas, 107.1 km^2 (1.1-770 km^2; SD = 165.9 km^2).

FIG. 5 Home range size, in log scale, from 2017-2023, with the dry and wet seasons of each year coloured in lighter orange and blue. Each point represents the fortnightly estimate of individuals' home range. The Confidence Intervals are shown around each estimate.

FIG. 6 Core area size, in log scale, from 2017-2023, with the dry and wet seasons of each year coloured in lighter orange and blue. Each point represents the fortnightly estimate of individuals' core area. The Confidence Intervals are shown around each estimate.

Home range and core area size model

The temporal variation in fortnightly home range size of juvenile Lear's macaws was best explained by season and site (Supplementary Table 6), indicating that macaws tend to have variable home range sizes depending on the site – larger in *Estação Biológica de Canudos* roosting site, smaller in *Boqueirão da Onça* release area –, and larger home ranges in dry season. However, the adjusted R^2 value estimated for the selected model ($R^2 = 0.02256$) indicated that these predictor variables represented only ~2.25% of the temporal variation observed in the sizes of the macaws' home ranges. Also, other equally plausible models were selected (dAIC < 2; Supplementary Table 6), including the null model – therefore indicating only a slight influence of these variables on the home ranges size temporal variation.

Regarding the core areas, their temporal variation was linked to the accumulated rainfall over the last six months (Supplementary Table 7). However, the adjusted R^2 value estimated for the top model ($R^2 = 0.01699$) indicated that this predictor variable also represented only a small fraction (~1.7%) of the temporal variation observed in the fortnightly sizes of the macaws' core areas; additionally, other equally plausible models were selected (dAIC < 2; Supplementary Table 7).

Discussion

Our findings provide the first comprehensive estimates of Lear's macaw home ranges and core areas, offering novel insights into their spatial ecology and habitat use. Spatial distribution analysis of feeding, resting, and roosting sites demonstrated that macaws predominantly utilize areas outside protected zones, with roosting sites concentrated near sandstone cliffs; while feeding and resting sites are often in anthropogenically modified landscapes, scattered across individuals' ranges – providing empirical evidence for key habitats in need of restoration and conservation. We also found significant inter and intra-annual variation in home range sizes, with larger ranges during the dry season. We observed that, while tagging site and season influenced home range variation, the environmental productivity proxies – NDVI and rainfall – did not strongly explain the temporal fluctuations. These results underscore the complexity of factors influencing macaws' space use, suggesting a multifaceted interaction between rainfall, landscape composition and configuration and food availability (McIntyre & Wiens, 2000; Adamek, 2011).

Deploying GPS tags on Lear's macaws presented logistical challenges but yielded valuable long-term movement data (Supplementary Table 4). Of the 38 tagged macaws, 44.7% experienced tag removal or destruction, highlighting the challenges associated with tracking of parrots in their natural habitats. This issue is common among parrot species that engage in preening and mutual preening behaviours (Le Souef et al., 2013; Groom et al., 2014). Therefore, understanding loss rates is crucial for planning future telemetry research, especially given the high cost of equipment. Additional factors may also contribute to data loss, such as tag malfunctions or the inability to locate tagged macaws during monitoring. Extended deployment periods, exceeding a year for some individuals, provided critical insights into seasonal and interannual movements. Ongoing refinement of harness attachment methods could further reduce logger loss and enhance data recovery rates in future studies (Brightsmith et al., 2021).

The spatial and temporal distribution of macaw activity hotspots revealed distinct patterns in the use of feeding, resting, and roosting sites. Roosting sites, primarily sandstone cliffs, remain critical despite new findings about tree roosts and served as stable nightly refuges while feeding and resting locations shifted more dynamically across the landscape. Interestingly, an amount of feeding and resting sites overlapped, suggesting that macaws utilize the same areas for multiple activities, thereby minimizing energy expenditure (Santos Neto & Camandaroba, 2008; Pacífico et al., 2014). These findings reflect the species' reliance on localized licuri palm patches, reinforcing the importance of conserving these fragmented but essential habitats.

Habitat characterization of feeding, resting, and roosting sites highlighted notable differences in landscape features. Feeding and resting sites were often situated closer to roads and power lines, with higher levels of human modification (HMc), compared to roosting sites. Roosting areas, on the other hand, were associated with steeper slopes and less disturbed habitats, underscoring the critical role of sandstone cliffs. These distinctions emphasize the macaws' ability to navigate anthropogenic landscapes for foraging while depending on more pristine environments for roosting, reflecting an adaptive spatial strategy in response to habitat fragmentation (Tuomainen & Candolin, 2011; Salinas-Melgoza et al., 2013; Renton et al., 2015).

Home range and core area estimates exhibited substantial variation across individuals. Also, the ranges' sizes were smaller for the reintroduced macaws (IDs 6444, 9015; Supplementary Table 3) than for the wild ones. The mean home range size of 850.15 km² aligns with estimates from other large macaws, although the observed variability (ranging 1.24-8,549.48 km²) highlights individual differences in space use (Brightsmith et al., 2021). This range disparity likely reflects differences in age, experience, and local resource distribution (Viana et al., 2018; Isted et al., 2023). Temporal variation in home range sizes, with larger ranges during dry season, supports the hypothesis that macaws expand their foraging areas in response to seasonal resource scarcity. This pattern mirrors findings on other tropical frugivores, where seasonal movements and dry-season range expansion is a common adaptive strategy (Salinas-Melgoza et al., 2013; Brightsmith et al., 2021). The variation in home range sizes over annual cycles has also been documented for other species and highlights the dynamic nature of home ranges (Chan et al., 2022; Isted et al., 2023; Broekman et al., 2024). Usually, animals tend to show smaller home ranges when habitats present higher productivity, leading to higher resource availability and so demanding smaller areas to find enough resources (Börger et al., 2008; Duncan et al., 2015). The spatiotemporal variation in resource availability is considered one of the key drivers of home range size variation (Broekman et al., 2024).

The licuri palm, a key resource for Lear's macaw, is influenced by rainfall patterns typical of the Caatinga dry forest (Pacífico et al., 2014). However, although the precipitation temporal scales we selected were based on its reproductive phenology, it is possible that its flowering and fructification are not immediately triggered by rainfall, as occurs with most Caatinga plants. During droughts, licuri palms may maintain vegetative growth, but fruit production can significantly decrease, further impacting macaw foraging behaviour (Griz & Machado, 2001; Alves et al., 2019; Noblick et al., 2020). Additionally, although NDVI is a well-established proxy for photosynthetic activity and green biomass (Pettorelli et al., 2005), its effectiveness as a proxy of licuri fruit availability may be limited, as palms can retain green foliage during different phenological stages, even during fruit-scarce periods (Alves et al., 2019). This discrepancy underscores the need for more tailored remote sensing techniques or ground-based phenological surveys to accurately capture the relationship between food availability and macaw space use.

The movement of macaws and variation in their home range sizes may be explained by multiple dynamic processes affecting their movement ecology (Isted et al., 2023). These factors can be both environmental and intrinsic, related to individuals' internal state (e.g., physiological restrictions) and/or individuals' traits (e.g., locomotion and/or navigation capacity; Nathan et al., 2008). Also, social interactions and other biotic factors may further shape macaw spatial use, highlighting the importance of incorporating diverse ecological drivers into future research.

Despite the observed variability in home range sizes, the consistent use of roosting and feeding areas emphasizes the residency pattern of Lear's macaws. This stability highlights the importance of restoring and protecting key areas that are critical for their survival, particularly licuri palm patches and sandstone cliffs, which serve as primary feeding and roosting sites. The reliance on fragmented landscapes and expansion of home ranges during dry seasons underline the macaws' adaptive strategies in response to resource scarcity (Salinas-Melgoza et al., 2013), reinforcing the need for long-term conservation planning that addresses both the amount of suitable habitat and the seasonal and interannual habitat dynamics. Conservation efforts should focus on restoring and preserving native Caatinga vegetation and controlling land conversion and vegetation degradation to reduce anthropogenic disturbances, ensuring that critical resources like licuri fruits remain available throughout the year and support the long-term persistence of Lear's macaw populations (Pacífico et al., 2014; Barbosa & Tella, 2019).

Monitoring through telemetry studies continues to be an essential tool to identify and protect priority areas, guiding targeted actions to mitigate habitat degradation and support the persistence of macaws' populations in the long-term.

Author contributions Study design: FRP, ECP, FVD, JEFO; fieldwork: FRP, ECP, TF, GRF; data analysis, writing: FRP, ECP, FVD, JEFO, PC; reviewing: all authors.

Acknowledgments This study was funded by *Fundação de Amparo à Pesquisa do estado de São Paulo* (FAPESP), FVD Young Investigator Grant nº 2018/19389-9, FRP Masters Scholarship nº 2021/14510-7, JEFO Post-Doctoral Fellowship nº 2021/02132-8. Fieldwork activities and tags were also partially funded by *Voltalia* and *Enel Green Power* (2019-2023). We thank Dr. José L. Tella, Manuel de la Riva, Dr. Martin Wikelski, Dr. Kamran Safi, Dr. Andrea Koelzsch and Dr. Paulo Roberto Guimarães for scientific support; Dorivaldo Alves, Guilherme Feitosa, João Carlos Nogueira, Máximo Cardoso and Marcelo Oliveira for field work assistance; the National Center for Wild Bird Research and Conservation (CEMAVE), Chico Mendes Institute for Biodiversity

Conservation (ICMBio), *Fundação Biodiversitas* and Environment Authority for the Bahia state (INEMA) for logistic support. We also thank all fieldwork volunteers.

Conflicts of interest None.

Ethical standards This study abided by the Oryx guidelines on ethical standards. The macaws were captured and tagged under appropriate licenses granted by the Brazilian Ethics Committee (permit nº 381/2021) and ICMBio (permits nº 12763 and 59505).

Data availability The data that supported our findings is stored in Movebank Data Repository hosted by Max Planck Institute of Animal Behavior (movebank.org, "(EBD) *Anodorhynchus leari* (Lear's Macaw) Study", study ID 322731302).

References

ADAMEK, K.A. (2011) *Temporal variation in space and resource use of macaws in the Southeastern Peruvian Amazon*. Masters' Dissertation, Texas A&M University, Texas, USA.

AKAIKE, H. (1987) Factor analysis and AIC. *Psychometrika*, 52, 317–332.

ANEEL (2024) *Agência Nacional de Energia Elétrica. Sistema de Informação Geográfico Regulatório da Distribuição (SIG-R)e Base de Dados Geográfica da Distribuidora - BDGD*. dadosabertos-aneel.opendata.arcgis.com/search?tags=distribuicao [accessed November 2024].

ALVES, H., KUMAR, T.V.L., PAREDES, F., ELLIOTT, S. & AYUGA, J.G. (2019) Assessment of Caatinga response to drought using Meteosat-SEVIRI Normalized Difference Vegetation Index (2008 – 2016). *ISPRS Journal of Photogrammetry and Remote Sensing*, 148, 235–252.

BARBOSA, A.E.A. & TELLA, J.L. (2019) How much does it cost to save a species from extinction? Costs and rewards of conserving the Lear's macaw. *Royal Society Open Science*, 6, 190190.

BirdLife International (2020) *Anodorhynchus leari* (amended version of 2019 assessment). *The IUCN Red List of Threatened Species 2020*. dx.doi.org/10.2305/IUCN.UK.2020-3.RLTS.T22685521A176030480.en [accessed October 2021].

Börger, L., Dalziel, B.D. & Fryxell, J.M. (2008) Are there general mechanisms of animal home range behaviour? A review and prospects for future research. *Ecology Letters*, 11, 637–650.

Brightsmith, D.J., Boyd, J.D., Hobson, E.A. & Randel, C.J. (2021) Satellite telemetry reveals complex migratory movement patterns of two large macaw species in the western Amazon basin. *Avian Conservation and Ecology*, 16, art14.

Broekman, M.J.E., Hilbers, J.P., Hoeks, S., Huijbregts, M.A.J., Schipper, A.M. & Tucker, M.A. (2024) Environmental drivers of global variation in home range size of terrestrial and marine mammals. *Journal of Animal Ecology*, 93, 488–500.

Burnham, K.P. & Anderson, D.R. (2002) Model Selection and Multimodel Inference: A Practical Information-Theoretic Approach. In *Sociological Methods and Research* p. 2nd edition. Springer-Verlag, New York, USA.

Calabrese, J.M., Fleming, C.H. & Gurarie, E. (2016) ctmm: an <scp>r</scp> package for analyzing animal relocation data as a continuous-time stochastic process. *Methods in Ecology and Evolution*, 7, 1124–1132.

Chan, A.N., Wittemyer, G., McEvoy, J., Williams, A.C., Cox, N., Soe, P., et al. (2022) Landscape characteristics influence ranging behavior of Asian elephants at the human-wildlands interface in Myanmar. *Movement Ecology*, 10, 6.

DNIT (2021) *Departamento Nacional de Infraestrutura de Transportes*. servicos.dnit.gov.br/vgeo [accessed October 2024].

Duncan, C., Nilsen, E.B., Linnell, J.D.C. & Pettorelli, N. (2015) Life-history attributes and resource dynamics determine intraspecific home-range sizes in Carnivora. *Remote Sensing in Ecology and Conservation*, 1, 39–50.

European Space Agency (2024) *Copernicus Global Digital Elevation Model*. Distributed by OpenTopography. https://doi.org/10.5069/G9028PQB [accessed November 2024].

Fernandes, M.F., Cardoso, D. & de Queiroz, L.P. (2020) An updated plant checklist of the Brazilian Caatinga seasonally dry forests and woodlands reveals high species richness and endemism. *Journal of Arid Environments*, 174, 104079.

Fleming, C.H., Drescher-Lehman, J., Noonan, M.J., Akre, T.S.B., Brown, D.J., Cochrane, M.M., et al. (2020) A comprehensive framework for handling location error in animal tracking data. Cold Spring Harbor Laboratory. *bioRxiv*.

Fleming, C.H., Fagan, W.F., Mueller, T., Olson, K.A., Leimgruber, P. & Calabrese, J.M. (2015) Rigorous home range estimation with movement data: a new autocorrelated kernel density estimator. *Ecology*, 96, 1182–1188.

Franca Rocha, W.J.S., Vasconcelos, R.N., Costa, D.P., Duverger, S.G., Lobão, J.S.B., Souza, D.T.M., et al. (2024) Towards Uncovering Three Decades of LULC in the Brazilian Drylands: Caatinga Biome Dynamics (1985–2019). *Land*, 13, 1250.

Goldingay, R.L. (2015) A review of home-range studies on Australian terrestrial vertebrates: adequacy of studies, testing of hypotheses, and relevance to conservation and international studies. *Australian Journal of Zoology*, 63, 136.

GPCA (2024) *Grupo de Pesquisa e Conservação da Arara-azul-de-lear (GPCA). Relatório anual 2023. São Paulo: 2024.* acrobat.adobe.com/id/urn:aaid:sc:VA6C2:dd788c72-bed4-4191-98ca-d5984143fcdf [accessed October 2024].

Griz, L.M.S. & Machado, I.C.S. (2001) Fruiting phenology and seed dispersal syndromes in caatinga, a tropical dry forest in the northeast of Brazil. *Journal of Tropical Ecology*, 17, 303–321.

Groom, C., Warren, K., Le Souef, A. & Dawson, R. (2014) Attachment and performance of Argos satellite tracking devices fitted to black cockatoos (Calyptorhynchus spp.). *Wildlife Research*, 41, 571.

Isted, G.H., Thomas, R.J., Warner, K.S., Stuber, M.J., Ellsworth, E. & Katzner, T.E. (2023) Ferruginous Hawk movements respond predictably to intra-annual variation but unexpectedly to anthropogenic habitats. *Ibis*, 165, 1156–1168.

Kays, R., Davidson, S.C., Berger, M., Bohrer, G., Fiedler, W., Flack, A., et al. (2022) The Movebank system for studying global animal movement and demography. *Methods in Ecology and Evolution*, 13, 419–431.

Kennedy, C.M., Oakleaf, J.R., Theobald, D.M., Baruch-Mordo, S. & Kiesecker, J. (2019) Managing the middle: A shift in conservation priorities based on the global human modification gradient. *Global Change Biology*, 25, 811–826.

Kölzsch, A., Lameris, T.K., Müskens, G.J.D.M., Schreven, K.H.T., Buitendijk, N.H., Kruckenberg, H., et al. (2023) Wild goose chase: Geese flee high and far, and with aftereffects from New Year's fireworks. *Conservation Letters*, 16.

MapBiomas (2024) *Coleção 8 da série anual de Mapas de Cobertura e Uso da Terra do Brasil.* brasil.mapbiomas.org [accessed November 2024].

McIntyre, N.E. & Wiens, J.A. (2000) A novel use of the lacunarity index to discern landscape function. *Landscape Ecology*, 15, 313–321.

Morato, R.G., Connette, G.M., Stabach, J.A., De Paula, R.C., Ferraz, K.M.P.M., Kantek, D.L.Z., et al. (2018) Resource selection in an apex predator and variation in response to local landscape characteristics. *Biological Conservation*, 228, 233–240.

Moro, M.F., Nic Lughadha, E., de Araújo, F.S. & Martins, F.R. (2016) A Phytogeographical Metaanalysis of the Semiarid Caatinga Domain in Brazil. *The Botanical Review*, 82, 91–148.

Nathan, R., Getz, W.M., Revilla, E., Holyoak, M., Kadmon, R., Saltz, D. & Smouse, P.E. (2008) A movement ecology paradigm for unifying organismal movement research. *Proceedings of the National Academy of Sciences*, 105, 19052–19059.

Noblick, L., Wintergerst, S., Noblick, D. & Lima, J.T. (2020) Syagrus coronata (Arecaceae) phenology and the impact of fire on survival and reproduction of the licuri palm. *SITIENTIBUS série Ciências Biológicas*, 20, 1–9.

Oliveira, M. da R., Szabo, J.K., Júnior, A. dos S., Guedes, N.M.R., Tomas, W.M., Camilo, A.R., et al. (2021) Lack of protected areas and future habitat loss threaten the Hyacinth Macaw (Anodorhynchus hyacinthinus) and its main food and nesting resources. *Ibis*, 163, 1217–1234.

Pacífico, E.C., Barbosa, E.A., Filadelfo, T., Oliveira, K.G., Silveira, L.F. & Tella, J.L. (2014) Breeding to non-breeding population ratio and breeding performance of the globally Endangered Lear's Macaw *Anodorhynchus leari* : conservation and monitoring implications. *Bird Conservation International*, 24, 466–476.

Pacífico, E.C., Efstathion, C.A., Filadelfo, T., Horsburgh, R., Cunha, R.A., Paschotto, F.R., et al. (2020) Experimental removal of invasive Africanized honey bees increased breeding population size of the endangered Lear's macaw. *Pest Management Science*, 76, 4141–4149.

Pettorelli, N., Vik, J.O., Mysterud, A., Gaillard, J.-M., Tucker, C.J. & Stenseth, N.C. (2005) Using the satellite-derived NDVI to assess ecological responses to environmental change. *Trends in Ecology & Evolution*, 20, 503–510.

QGIS Development Team (2023) *QGIS Geographic Information System*. Open-Source Geospatial Foundation. qgis.org

R Core Team (2023) *R: A Language and Environment for Statistical Computing.* R Foundation for Statistical Computing, Vienna, Austria. R-project.org/

Rencher, A.C. & Schaalje, G.B. (2008) *Linear Models in Statistics*. 2nd edition. John Wiley & Sons, New Jersey, USA.

Renton, K., Salinas-Melgoza, A., De Labra-Hernández, M.Á. & de la Parra-Martínez, S.M. (2015) Resource requirements of parrots: nest site selectivity and dietary plasticity of Psittaciformes. *Journal of Ornithology*, 156, 73–90.

Salinas-Melgoza, A., Salinas-Melgoza, V. & Wright, T.F. (2013) Behavioral plasticity of a threatened parrot in human-modified landscapes. *Biological Conservation*, 159, 303–312.

Santos Neto, J.R. dos & Camandaroba, M. (2008) Mapeamento dos sítios de alimentação da arara-azul-de-lear Anodorhynchus leari (Bonaparte, 1856). *Ornithologia*, 3, 1–17.

Schofield, G., Hobson, V.J., Lilley, M.K.S., Katselidis, K.A., Bishop, C.M., Brown, P. & Hays, G.C. (2010) Inter-annual variability in the home range of breeding turtles: Implications for current and future conservation management. *Biological Conservation*, 143, 722–730.

Silva, J.M.C., Leal, I.R. & Tabarelli, M. (2017) *Caatinga: The Largest Tropical Dry-Forest Region in South America*. Springer International Publishing, New York, USA.

Silva-Neto, G. F., Sousa, A. E. B. A. & dos Santos-Neto, J. R. (2012) Novas informações sobre a dieta da arara-azul-de-lear, *Anodorhynchus leari* Bonaparte, 1856 (Aves, Psittacidae). *Ornithologia*, *5*, 1–5.

Le Souef, A.T., Stojanovic, D., Burbidge, A.H., Vitali, S.D., Heinsohn, R., Dawson, R. & Warren, K.S. (2013) Retention of transmitter attachments on black cockatoos (Calyptorhynchus spp.). *Pacific Conservation Biology*, 19, 55.

Su, X., Yan, X. & Tsai, C. (2012) Linear regression. *WIREs Computational Statistics*, 4, 275–294.

Tuomainen, U. & Candolin, U. (2011) Behavioural responses to human-induced environmental change. *Biological Reviews*, 86, 640–657.

Viana, D.S., Granados, J.E., Fandos, P., Pérez, J.M., Cano-Manuel, F.J., Burón, D., et al. (2018) Linking seasonal home range size with habitat selection and movement in a mountain ungulate. *Movement Ecology*, 6, 1.

Walton, Z., Samelius, G., Odden, M. & Willebrand, T. (2017) Variation in home range size of red foxes Vulpes vulpes along a gradient of productivity and human landscape alteration. *PLOS ONE*, 12, e0175291.

Yeap, L., Shephard, J., Bouten, W., Jackson, B., Vaughan-Higgins, R. & Warren, K. (2017) Development of a tag-attachment method to enable capture of fine- and landscape-scale movement in black-cockatoos. *Australian Field Ornithology*, 34, 49–55.

YEAP, L., WARREN, K.S., BOUTEN, W., VAUGHAN-HIGGINS, R., JACKSON, B., RILEY, K., ET AL. (2021) Application of tri-axial accelerometer data to the interpretation of movement and behaviour of threatened black cockatoos. *Wildlife Research*, 49, 100–110.

Revealing the unknown world of the endangered Lear's macaw using GPS-tracking data: identification of critical habitats for conservation

FERNANDA R. PASCHOTTO, ERICA C. PACÍFICO, THIAGO FILADELFO, GABRIELA R. FAVORETTO, JULIA E. F. OSHIMA, PAULO CARDOSO, FRANCISCO V. DÉNES

SUPPLEMENTARY MATERIAL 1 Details on tag deployment and GPS data collection.

In *Raso da Catarina* region, we deployed tags on 29 wild immature macaws (pre-fledging, approximately 3-months-old) captured inside their nests over seven breeding seasons between 2017 and 2023. Before the individual's capture, direct observations using telescopes and binoculars were undertaken to identify the nests occupied by breeding pairs (Pacífico et al., 2014). The cavity nests in the sandstone cliffs were accessed through rappel techniques, according to Pacífico et al. (2014), selecting the nestlings in the appropriate stage of development to receive the bio-loggers.

In *Boqueirão da Onça*, the release area, tags were deployed on seven captive-bred (two to five years old) and two rescued macaws (two and four years old) released between 2019 and 2022, after four months of training and adaptation in the release area. Tags were deployed during pre-release management conducted a few days prior to release, allowing behavioral observations of the tagged individuals both before and after the release.

Tags were programmed to record GPS locations at 10-min or 30-min intervals, between 4 am-7 pm (local time) every day year-round (frequency of GPS fixes depended on the available solar-powered battery charge).

SUPPLEMENTARY MATERIAL 2 MoveApps workflow analysis protocol performed for identification of feeding, resting and roosting sites.

To perform the identification of the feeding, resting and roosting sites, we accessed the "Roost and Foraging Site Extraction" workflow (Kölzsch, 2022) in the MoveApps (moveapps.org/workflows), a free platform for analysis of animal movement data. The Apps extracted, from the movement tracks, the mean coordinates of daily diurnal and/or nocturnal locations – depending on your settings – of high GPS fix density where the animals stayed in a certain radius area for a defined minimum duration, not moving faster than 1 m/s (GPS ground speed). The locations are given as .csv file output.

Within the main workflow "Roost and Foraging Site Extraction", there are two available workflows: the 'Foraging site extraction (day)', with combined Apps to extract stationary locations during day; and the 'Roost site extraction (night)' to extract stationary locations during night. Be aware that there may be available more recent versions of the Apps within the workflows by the time you will use it. It is possible to upgrade the workflows and use the latest version.

We extracted both the feeding and resting sites running the analysis of 'Foraging site extraction (day)' workflow, changing a few parameters among them (detailed below); and extracted the roosting sites running the analysis of 'Roost site extraction (night)' workflow.

App 'Movebank Location' settings:

After adding the respective two workflows in our personal profile within the MoveApps platform, the next step (i.e., first App) was the selection of a data source, by configuring our Movebank login details to directly download the movement data stored in this platform – alternatively, it is also possible to upload movement-based files from a Cloud Storage or local systems.

We configured the Movebank location data source by providing the Movebank login, the study name, the animals for which we wanted to analyze the movement data, and the sensor types (GPS sensor). In this step, other settings were also requested. We chose to: not include outliers in this analysis, not use fast data reduction profile, and not use argument of minimization. Also, we selected a full data resolution, and the attribute of the defining track ID was a combination of animal and deployment. We repeated this procedure for both the 'Foraging site extraction (day)' and 'Roost site extraction (night)' workflows.

We saved the changes after configuring the parameters within each App.

App 'Filter/Annotate by Season' settings:

This App makes it possible to filter the data by season, comparing positions in different time intervals. In our study, we did not provide any time range to annotate positions to filter the data.

App 'Daily Rest/Foraging Sites' settings:

In both 'Foraging site extraction (day)' and 'Roost site extraction (night)' workflows, all GPS fixes were classified as day or night positions, delineated by sunrise +30 min ('Sunrise adaptation time') and by sunset -60 min ('Sunset adaptation time'), as macaws tend to leave roosting sites about 30 min after sunrise, and stay at foraging sites until about 60 min before sunset; E.C.P. field observation, 2008). These settings depend on each species' behavior.

For all the analysis, the ‘Maximum resting speed’ inserted was 1 m/s GPS ground speed (analysis default). Feeding sites were defined as all sites at daylight where a macaw stayed for at least 5 h (‘Minimum resting duration’) within a radius of 1,000 m (‘‘Maximum resting radius’). The resting sites were defined as all sites during daytime where a macaw stayed for at least 3 h (‘Minimum resting duration’) within a radius of 50 m (‘Maximum resting radius’). Lastly, the roosting sites were defined as all sites during nighttime where a macaw stayed for at least 9 h (‘Minimum resting duration’) within a radius of 500 m (‘Maximum resting radius’).

Radii and time intervals selected to identify feeding, resting and roosting sites were established considering the species’ movements and observed behavior.

Output:

The identified locations were given as .csv files output.

More detailed documentation of the Daily Rest/Foraging Sites MoveApps is available on the authors’ GitHub repository.

SUPPLEMENTARY TABLE 1 Detailed information of the environmental variables ‘Distance from roads’, ‘Human modification’, ‘Distance from power lines’, ‘Land cover and land use’ and ‘Slope’ used for habitat characterization.

Variable	**Type of information**	**Institution**	**Description**	**Unit**	**Year of original database**	**Original pixel resolution**	**Final pixel resolution**	**Primary or derived**	**Derived from**	**Source**
Distance from roads	Anthropic	Departamento Nacional de Infraestrutura de Transportes (DNIT)	Raster with Euclidean distance calculated from roads shapefile	Meters	2021-2022	Vector	30m	Derived	Roads	Departamento Nacional de Infraestrutura de Transportes (DNIT) 2021. Visualizador de Informações Geográficas - Base oficial das rodovias federais e estaduais.
Human modification	Anthropic	The Nature Conservancy	Raster with values of human modification. It is a continuous 0-1 metric that reflects the proportion of a landscape modified based on modeling the physical extents of 13 anthropogenic stressors and their estimated impacts using spatially explicit global datasets with a median year of 2016	NA	2016	1km	30m	Primary	NA	Kennedy, C. M., Oakleaf, J. R., Theobald, D. M., Baruch-Mordo, S., & Kiesecker, J. (2019). Managing the middle: A shift in conservation priorities based on the global human modification gradient. Global change biology, 25(3), 811-826.
Distance from power lines	Anthropic	Agência Nacional de Energia Elétrica (ANEEL)	Raster with Euclidean distance calculated from medium voltage network	Meters	2020	Vector	30m	Derived	Medium voltage network	Agência Nacional de Energia Elétrica (ANEEL) 2024. Sistema de Informação Geográfico Regulatório da distribuição (SIG-R)e Base de Dados Geográfica da Distribuidora - BDGD
Land cover	Landscape	MapBiomas	Raster with values of land use and land cover classification	Land cover class	2016	30m	30m	Primary	NA	“MapBiomas - Coleção 8 da série anual de Mapas de Cobertura e uso da terra do Brasil, acessado em 2024 através do link: https://brasil.mapbiomas.org/”
Slope	Topography	European Space Agency	Raster with mean slope values derived from the Copernicus Digital Elevation Model	Degrees	2011-2015	30m	30m	Derived	Digital Elevation Model	European Space Agency (2021). Copernicus Global Digital Elevation Model. Distributed by OpenTopography. https://doi.org/10.5069/G9028PQB.

SUPPLEMENTARY TABLE 2 Summary of the fortnightly movement data series with identification of the Lear's Macaws ("ID") and the subsets, the beginning and end date of each subset (format year-month-day), the duration (in days) of the subsets, the number of points (i.e., geographic coordinates) registered for each subset, and the movement model selected.

* Subsets that recorded less than 15 days of movement data.

ID	Subset	Beginning date	End date	Duration (days)	Number of points	Selected model
5568	s1	2017-05-03	2017-05-17	15	1,339	OUF anisotropic
5568	s2	2017-05-18	2017-06-01	15	1,364	OUF anisotropic
5568	s3	2017-06-02	2017-06-16	15	1,364	OUF anisotropic
5568	s4	2017-06-17	2017-07-01	15	1,358	OUF anisotropic
5568	s5	2017-07-02	2017-07-16	15	1,365	OUF anisotropic
5568	s6	2017-07-17	2017-07-31	15	1,363	OUF anisotropic
5568	s7	2017-08-01	2017-08-15	15	1,357	OUF anisotropic
5568	s8	2017-08-16	2017-08-30	15	1,364	OUF anisotropic
5568	s9	2017-08-31	2017-09-14	15	1,354	OUF anisotropic
5568	s10	2017-09-15	2017-09-29	15	1,348	OUF anisotropic
5568	s11	2017-09-30	2017-10-14	15	1,358	OUF anisotropic
5568	s12	2017-10-15	2017-10-29	15	1,360	OUF anisotropic
5568	s13	2017-10-30	2017-11-13	15	1,360	OUF anisotropic
5568	s14	2017-11-14	2017-11-28	15	1,365	OUF anisotropic
5568	s15	2017-11-29	2017-12-13	15	1,358	OUF anisotropic
5568	s16	2017-12-14	2017-12-28	15	1,349	OUF anisotropic
5568	s17	2017-12-29	2018-01-12	15	1,353	OUF anisotropic
5568	s18	2018-01-13	2018-01-27	15	1,363	OUF anisotropic
5568	s19	2018-01-28	2018-02-11	15	1,362	OUF anisotropic
5568	s20	2018-02-12	2018-02-26	15	1,360	OUF anisotropic
5568	s21	2018-02-27	2018-03-13	15	1,362	OUF anisotropic
5568	s22	2018-03-14	2018-03-28	15	1,353	OUF anisotropic
5568	s23	2018-03-29	2018-04-12	15	1,349	OUF anisotropic
5568	s24	2018-04-13	2018-04-27	15	1,356	OUF anisotropic
5568	s25	2018-04-28	2018-05-12	15	1,365	OUF anisotropic
5568	s26	2018-05-13	2018-05-27	15	1,346	OUF anisotropic
5568	s27	2018-05-28	2018-06-11	15	1,359	OUF anisotropic
5568	s28	2018-06-12	2018-06-26	15	1,348	OUF anisotropic
5568	s29	2018-06-27	2018-07-11	15	1,364	OUF anisotropic
5568	s30	2018-07-12	2018-07-26	15	1,358	OUF anisotropic
5568	s31	2018-07-27	2018-08-10	15	1,365	OUF anisotropic
5568	s32	2018-08-11	2018-08-25	15	1,365	OUF anisotropic
5568	s33	2018-08-26	2018-09-09	15	1,365	OUF anisotropic
5568	s34	2018-09-10	2018-09-24	15	1,365	OUF anisotropic
5568	s35	2018-09-25	2018-10-09	15	1,362	OUF anisotropic
5568	s36	2018-10-10	2018-10-24	15	1,362	OUF anisotropic
5568	s37	2018-10-25	2018-11-08	15	1,362	OUF anisotropic
5568	s38	2018-11-09	2018-11-23	15	1,362	OUF anisotropic
5568	s39	2018-11-24	2018-12-08	15	1,365	OUF anisotropic
5568	s40	2018-12-09	2018-12-23	15	1,361	OUF anisotropic

ID	Subset	Beginning date	End date	Duration (days)	Number of points	Selected model
5568	s41	2018-12-24	2019-01-07	15	1,363	OUF anisotropic
5568	s42	2019-01-08	2019-01-22	15	1,362	OUF anisotropic
5568	s43	2019-01-23	2019-02-06	15	1,364	OUF anisotropic
5568	s44	2019-02-07	2019-02-21	15	1,365	OUF anisotropic
5568	s45	2019-02-22	2019-03-08	15	1,358	OUF anisotropic
5568	s46	2019-03-09	2019-03-23	15	1,362	OUF anisotropic
5568	s47	2019-03-24	2019-04-07	15	1,362	OUF anisotropic
5568	s48	2019-04-08	2019-04-22	15	1,365	OUF anisotropic
5568	s49	2019-04-23	2019-05-07	15	1,362	OUF anisotropic
5568	s50	2019-05-08	2019-05-22	15	1,363	OUF anisotropic
5568	s51	2019-05-23	2019-06-06	15	1,364	OUF anisotropic
5568	s52	2019-06-07	2019-06-21	15	1,363	OUF anisotropic
5568	s53	2019-06-22	2019-07-06	15	1,362	OUF anisotropic
5568	s54	2019-07-07	2019-07-21	15	1,362	OUF anisotropic
5570	s1	2017-05-03	2017-05-17	15	1,329	OUF anisotropic
5570	s2	2017-05-18	2017-06-01	15	1,344	OUF anisotropic
5570	s3	2017-06-02	2017-06-16	15	1,293	OUF anisotropic
5570	s4	2017-06-17	2017-07-01	15	1,105	OUF anisotropic
5570	s5	2017-07-02	2017-07-16	15	1,072	OUF anisotropic
5570	s6	2017-07-17	2017-07-31	15	1,136	OUF anisotropic
5570	s7	2017-08-01	2017-08-15	15	1,188	OUF anisotropic
5570	s8	2017-08-16	2017-08-30	15	1,163	OUF anisotropic
5570	s9	2017-08-31	2017-09-14	15	1,115	OUF anisotropic
5570	s10	2017-09-15	2017-09-29	15	1,106	OUF anisotropic
5570	s11	2017-09-30	2017-10-14	15	1,183	OUF anisotropic
5570	s12	2017-10-15	2017-10-29	15	1,246	OUF anisotropic
5570	s13	2017-10-30	2017-11-13	15	840	OUF anisotropic
5570	s14	2017-11-14	2017-11-28	15	1,085	OUF anisotropic
5570	s15	2017-11-29	2017-12-13	15	940	OUF anisotropic
5570	s16	2017-12-14	2017-12-28	15	811	OUF anisotropic
5570	s17	2017-12-29	2018-01-12	15	753	OUF anisotropic
5570	s18	2018-01-13	2018-01-27	15	1,144	OUF anisotropic
5570	s19	2018-01-28	2018-02-11	15	1,144	OUF anisotropic
5570	s20	2018-02-12	2018-02-26	15	949	OUF anisotropic
5570	s21	2018-02-27	2018-03-13	15	950	OUF anisotropic
5570	s22	2018-03-14	2018-03-28	15	1,028	OUF anisotropic
5570	s23	2018-03-29	2018-04-12	15	1,035	OUF anisotropic
5570	s24	2018-04-13	2018-04-27	15	1,026	OUF anisotropic
5570	s25	2018-04-28	2018-05-12	15	1,234	OUF anisotropic
5570	s26	2018-05-13	2018-05-27	15	940	OUF anisotropic
5570	s27	2018-05-28	2018-06-11	15	1,238	OUF anisotropic
5570	s28	2018-06-12	2018-06-26	15	1,126	OUF anisotropic
5570	s29	2018-06-27	2018-07-11	15	1,051	OUF anisotropic
5570	s30	2018-07-12	2018-07-26	15	1,222	OUF anisotropic
5570	s31	2018-07-27	2018-08-10	15	1,144	OUF anisotropic
5570	s32	2018-08-11	2018-08-25	15	1,105	OUF anisotropic
5570	s33	2018-08-26	2018-09-09	15	1,180	OUF anisotropic

ID	Subset	Beginning date	End date	Duration (days)	Number of points	Selected model
5570	s34	2018-09-10	2018-09-24	15	941	OUF anisotropic
5570	s35	2018-09-25	2018-10-09	15	1,015	OUF anisotropic
5570	s36	2018-10-10	2018-10-24	15	952	OUF anisotropic
5570	s37	2018-10-25	2018-11-08	15	1,228	OUF anisotropic
5570	s38	2018-11-09	2018-11-23	15	799	OUF anisotropic
5570	s39	2018-11-24	2018-12-08	15	929	OUF anisotropic
5570	s40	2018-12-09	2018-12-23	15	1,012	OUF anisotropic
5570	s41	2018-12-24	2019-01-07	15	806	OUF anisotropic
5570	s42	2019-01-08	2019-01-22	15	961	OUF anisotropic
5570	s43	2019-01-23	2019-02-06	15	929	OUF anisotropic
5570	s44	2019-02-07	2019-02-21	15	1,223	OUF anisotropic
5570	s45	2019-02-22	2019-03-08	15	871	OUF anisotropic
5570	s46	2019-03-09	2019-03-23	15	807	OUF anisotropic
5570	s47	2019-03-24	2019-04-07	15	972	OUF anisotropic
5570	s48	2019-04-08	2019-04-22	15	732	OUF anisotropic
5570	s49	2019-04-23	2019-05-07	15	599	OUF
5570	s50	2019-05-08	2019-05-22	15	407	OUF anisotropic
5570	s51	2019-05-23	2019-06-06	15	456	OUF anisotropic
5570	s52	2019-06-07	2019-06-21	15	556	OUF anisotropic
5570	s53	2019-06-22	2019-07-06	15	606	OUF anisotropic
5570	s54	2019-07-07	2019-07-21	15	426	OUF anisotropic
5570	s55	2019-07-22	2019-08-05	15	390	OUF anisotropic
5570	s56	2019-08-06	2019-08-20	15	687	OUF anisotropic
5570	s57	2019-08-21	2019-09-04	15	671	OUF anisotropic
5573	s1*	2018-06-26	2018-06-30	5	419	OUF anisotropic
5574	s1*	2018-07-07	2018-07-12	6	178	OU anisotropic
6444	s1	2021-02-09	2021-02-23	15	281	OU anisotropic
6444	s2	2021-02-24	2021-03-10	15	463	OU anisotropic
6444	s3	2021-03-11	2021-03-25	15	465	OU anisotropic
6444	s4	2021-03-26	2021-04-09	15	265	OU anisotropic
6444	s5	2021-04-10	2021-04-24	15	306	OUf anisotropic
6444	s6	2021-04-25	2021-05-09	15	298	OU anisotropic
6444	s7	2021-05-10	2021-05-24	15	12	OU anisotropic
6444	s8	2021-05-25	2021-06-08	15	83	IID anisotropic
6444	s10	2021-06-24	2021-07-08	15	1,185	OUF anisotropic
6444	s11	2021-07-09	2021-07-23	15	1,220	OUF anisotropic
6444	s12	2021-07-24	2021-08-07	15	2,071	OUF anisotropic
6444	s13	2021-08-08	2021-08-22	15	4,570	OUF anisotropic
6444	s14	2021-08-23	2021-09-06	15	4,800	OUF anisotropic
6444	s15	2021-09-07	2021-09-21	15	4,711	OUF anisotropic
6444	s16	2021-09-22	2021-10-06	15	4,705	OUF anisotropic
6444	s17	2021-10-07	2021-10-21	15	4,573	OUF anisotropic
6444	s18	2021-10-22	2021-11-05	15	4,391	OUF anisotropic
6444	s19	2021-11-06	2021-11-20	15	4,741	OUF anisotropic
6444	s20	2021-11-21	2021-12-05	15	4,735	OUF anisotropic
6444	s21	2021-12-06	2021-12-20	15	4,525	OUF anisotropic
6444	s22	2021-12-21	2022-01-04	15	4,398	OUF anisotropic

ID	Subset	Beginning date	End date	Duration (days)	Number of points	Selected model
6444	s23	2022-01-05	2022-01-19	15	4,797	OUF anisotropic
6444	s24	2022-01-20	2022-02-03	15	4,415	OUF anisotropic
6444	s25	2022-02-04	2022-02-18	15	4,127	OUF anisotropic
6444	s26	2022-02-19	2022-03-05	15	2,680	OUF anisotropic
6444	s27	2022-03-06	2022-03-20	15	4,369	OUF anisotropic
6444	s28	2022-03-21	2022-04-04	15	4,590	OUF anisotropic
6444	s29	2022-04-05	2022-04-19	15	4,314	OUF anisotropic
6444	s30	2022-04-20	2022-05-04	15	4,571	OUF anisotropic
6444	s31	2022-05-05	2022-05-19	15	4,516	OUF anisotropic
6444	s32	2022-05-20	2022-06-03	15	4,883	OUF anisotropic
6444	s33	2022-06-04	2022-06-18	15	4,660	OUF anisotropic
6444	s34	2022-06-19	2022-07-03	15	4,629	OUF anisotropic
6444	s35	2022-07-04	2022-07-18	15	4,313	OUF anisotropic
6444	s36	2022-07-19	2022-08-02	15	7,427	OUF anisotropic
6444	s37	2022-08-03	2022-08-17	15	9,244	OUF anisotropic
6444	s38	2022-08-18	2022-09-01	15	10,528	OUF anisotropic
6444	s39	2022-09-02	2022-09-16	15	11,892	OUF anisotropic
6444	s40	2022-09-17	2022-10-01	15	12,455	OUF anisotropic
6444	s41	2022-10-02	2022-10-16	15	12,535	OUF anisotropic
6444	s42	2022-10-17	2022-10-31	15	12,002	OUF anisotropic
6444	s43	2022-11-01	2022-11-15	15	10,855	OUF anisotropic
6444	s44	2022-11-16	2022-11-30	15	12,673	OUF anisotropic
6444	s45	2022-12-01	2022-12-15	15	10,742	OUF
6444	s46	2022-12-16	2022-12-30	15	11,157	OUF anisotropic
6444	s47	2022-12-31	2023-01-14	15	11,442	OUF anisotropic
6444	s48	2023-01-15	2023-01-29	15	11,044	OUF anisotropic
6444	s49	2023-01-30	2023-02-13	15	11,130	OUF anisotropic
6444	s50	2023-02-14	2023-02-28	15	9,784	OUF anisotropic
9015	s1	2021-02-09	2021-02-23	15	805	OU anisotropic
9015	s2	2021-02-24	2021-03-10	15	1,365	OU anisotropic
9024	s1*	2021-07-09	2021-07-21	13	1,154	OUF anisotropic
9026	s1	2022-04-29	2022-05-13	15	1,338	OUF anisotropic
9250	s1	2022-04-30	2022-05-14	15	2,043	OUF anisotropic
9250	s2*	2022-05-15	2022-05-20	6	313	OUF anisotropic
9252	s1*	2022-06-27	2022-06-30	4	696	OUF anisotropic
9025	s1	2021-07-09	2021-07-23	15	1,330	OUF anisotropic
9025	s2	2021-07-24	2021-08-07	15	1,333	OUF anisotropic
9025	s3	2021-08-08	2021-08-22	15	1,295	OUF anisotropic
9025	s4	2021-08-23	2021-09-06	15	1,276	OUF anisotropic
9025	s5	2021-09-07	2021-09-21	15	1,292	OUF anisotropic
9025	s6	2021-09-22	2021-10-06	15	1,301	OUF anisotropic
9025	s7	2021-10-07	2021-10-21	15	1,317	OUF anisotropic
9025	s8	2021-10-22	2021-11-05	15	1,302	OUF anisotropic
9025	s9	2021-11-06	2021-11-20	15	1,261	OUF anisotropic
9025	s10	2021-11-21	2021-12-05	15	1,215	OUF anisotropic
9025	s11	2021-12-06	2021-12-20	15	1,219	OUF anisotropic
9025	s12	2021-12-21	2022-01-04	15	1,277	OUF anisotropic

ID	Subset	Beginning date	End date	Duration (days)	Number of points	Selected model
9025	s13	2022-01-05	2022-01-19	15	1,277	OUF anisotropic
9025	s14	2022-01-20	2022-02-03	15	1,257	OUF anisotropic
9025	s15	2022-02-04	2022-02-18	15	1,253	OUF anisotropic
9025	s16	2022-02-19	2022-03-05	15	1,185	OUF anisotropic
9025	s17	2022-03-06	2022-03-20	15	1,231	OUF anisotropic
9025	s18	2022-03-21	2022-04-04	15	1,204	OUF anisotropic
9025	s19	2022-04-05	2022-04-19	15	1,223	OUF anisotropic
9025	s20	2022-04-20	2022-05-04	15	1,229	OUF anisotropic
9025	s21	2022-05-05	2022-05-19	15	1,214	OUF anisotropic
9025	s22	2022-05-20	2022-06-03	15	1,126	OUF anisotropic
9025	s23	2022-06-04	2022-06-18	15	934	OUF anisotropic
9025	s24	2022-06-19	2022-07-03	15	666	OUF anisotropic
9025	s25	2022-07-04	2022-07-18	15	625	OUF anisotropic
9025	s26	2022-07-19	2022-08-02	15	458	OUF anisotropic
9025	s27	2022-08-03	2022-08-17	15	359	OUF anisotropic
9025	s28	2022-08-18	2022-09-01	15	383	OUF anisotropic
9025	s34	2022-11-16	2022-11-30	15	345	OUF anisotropic
9025	s35	2022-12-01	2022-12-15	15	389	OUF anisotropic
9025	s36	2022-12-16	2022-12-30	15	327	OUF anisotropic
9025	s37	2022-12-31	2023-01-14	15	352	OUF anisotropic
9025	s38	2023-01-15	2023-01-29	15	403	OUF anisotropic
9025	s39	2023-01-30	2023-02-13	15	297	OUF anisotropic
9025	s40	2023-02-14	2023-02-28	15	283	OUF anisotropic
9025	s41	2023-03-01	2023-03-15	15	200	OU anisotropic
9025	s42	2023-03-16	2023-03-30	15	100	OUF anisotropic
9025	s43	2023-03-31	2023-04-14	15	92	OUf anisotropic
9025	s44	2023-04-15	2023-04-29	15	77	OUF anisotropic
9025	s45	2023-04-30	2023-05-14	15	138	OUF anisotropic
9025	s46	2023-05-15	2023-05-29	15	234	OUF anisotropic

SUPPLEMENTARY TABLE 3 Estimated home ranges and core areas (“Estimated 95%” and “Estimated 50%”, corresponding to the estimates, in km^2, of the 95% and 50% AKDE areas, respectively), for each fortnightly subset of macaw movement data (“Subset”), with identification of the individual (“ID”), the tagging site (*Estação Biológica de Canudos* (EBC), *Barreiras* and *B. do Chico* are breeding sites located in the *Raso da Catarina* region, and BDO is the release area in the *Boqueirão da Onça* region), the year of the respective fortnightly subset, the Confidence Intervals (CI) of each estimation (“Lower CI 95%” and “Upper CI 95%”, and “Lower CI 50%” and “Upper CI 50%”, corresponding to the CI lower and upper values, in km^2, of the 95% and 50% AKDE estimated areas, respectively), and the scaled home ranges and core areas (“Scaled est. 95%” and “Scaled est. 50%”, corresponding to the scaled variables “Estimated 95%” and “Estimated 50%”, respectively).

* Fortnightly estimates calculated using subsets with less than 15 days of movement data.

ID	Tagging site	Year	Subset	Estimated 95%	Lower CI 95%	Upper CI 95%	Estimated 50%	Lower CI 50%	Upper CI 50%	Scale est. 95%	Scaled est. 50%
5568	EBC	2017	s1	1,328.43	770.60	2,035.67	321.29	186.38	492.35	0.17	0.30
5568	EBC	2017	s2	1,312.42	897.17	1,805.40	342.39	234.06	471.00	0.15	0.39
5568	EBC	2017	s3	2,064.92	1,336.92	2,948.64	593.45	384.23	847.43	1.04	1.57
5568	EBC	2017	s4	673.26	457.95	929.41	157.39	107.05	217.26	-0.60	-0.47
5568	EBC	2017	s5	1,377.83	879.67	1,985.97	281.19	179.53	405.30	0.23	0.11
5568	EBC	2017	s6	960.46	631.39	1,357.46	169.41	111.36	239.43	-0.26	-0.41
5568	EBC	2017	s7	1,235.04	833.57	1,714.18	226.84	153.10	314.84	0.06	-0.14
5568	EBC	2017	s8	2,327.02	1,474.03	3,371.63	388.47	246.07	562.86	1.35	0.61
5568	EBC	2017	s9	2,172.70	1,360.77	3,171.53	613.00	383.93	894.81	1.17	1.66
5568	EBC	2017	s10	2,310.95	1,493.58	3,303.86	698.33	451.33	998.36	1.33	2.06
5568	EBC	2017	s11	838.61	578.89	1,145.70	164.84	113.79	225.20	-0.41	-0.43
5568	EBC	2017	s12	513.49	338.36	724.56	117.04	77.12	165.15	-0.79	-0.66
5568	EBC	2017	s13	834.95	568.37	1,151.98	162.81	110.83	224.63	-0.41	-0.44
5568	EBC	2017	s14	432.09	311.98	571.45	112.74	81.40	149.10	-0.89	-0.68
5568	EBC	2017	s15	714.43	482.91	990.57	151.69	102.54	210.33	-0.55	-0.49
5568	EBC	2017	s16	856.43	486.00	1,330.08	149.22	84.68	231.75	-0.39	-0.51
5568	EBC	2018	s17	615.68	416.33	853.41	123.55	83.54	171.25	-0.67	-0.63
5568	EBC	2018	s18	2,064.33	1,065.47	3,387.99	484.31	249.97	794.85	1.04	1.06
5568	EBC	2018	s19	1,598.39	1,029.02	2,291.14	311.70	200.67	446.79	0.49	0.25
5568	EBC	2018	s20	888.47	535.13	1,329.94	195.80	117.93	293.10	-0.35	-0.29
5568	EBC	2018	s21	114.91	77.14	160.09	17.37	11.66	24.19	-1.26	-1.12

ID	Tagging site	Year	Subset	Estimated 95%	Lower CI 95%	Upper CI 95%	Estimated 50%	Lower CI 50%	Upper CI 50%	Scale est. 95%	Scaled est. 50%
5568	EBC	2018	s22	1,178.40	699.83	1,779.61	165.79	98.46	250.38	-0.01	-0.43
5568	EBC	2018	s23	928.05	605.27	1,318.70	111.91	72.99	159.01	-0.30	-0.68
5568	EBC	2018	s24	1,749.35	927.45	2,827.70	342.22	181.44	553.18	0.67	0.39
5568	EBC	2018	s25	403.92	226.39	631.99	83.47	46.78	130.60	-0.92	-0.81
5568	EBC	2018	s26	1,716.65	962.48	2,685.43	363.45	203.77	568.56	0.63	0.49
5568	EBC	2018	s27	991.56	586.08	1,501.92	201.19	118.92	304.75	-0.23	-0.26
5568	EBC	2018	s28	1,749.45	1,200.53	2,400.09	383.69	263.30	526.39	0.67	0.59
5568	EBC	2018	s29	1,495.68	1,065.28	1,997.96	426.13	303.51	569.24	0.37	0.79
5568	EBC	2018	s30	1,342.91	927.71	1,833.67	323.28	223.33	441.42	0.19	0.31
5568	EBC	2018	s31	1,581.81	1,129.96	2,108.47	380.36	271.71	507.00	0.47	0.57
5568	EBC	2018	s32	4,763.80	2,443.15	7,846.32	1,116.04	572.37	1,838.20	4.22	4.00
5568	EBC	2018	s33	219.26	146.40	306.61	39.97	26.69	55.90	-1.14	-1.02
5568	EBC	2018	s34	748.20	466.30	1,095.68	139.43	86.90	204.18	-0.52	-0.55
5568	EBC	2018	s35	980.70	678.23	1,338.07	186.73	129.14	254.78	-0.24	-0.33
5568	EBC	2018	s36	611.51	461.57	782.23	127.12	95.95	162.61	-0.68	-0.61
5568	EBC	2018	s37	374.03	279.74	481.80	100.75	75.35	129.78	-0.96	-0.73
5568	EBC	2018	s38	581.25	430.90	753.75	143.19	106.15	185.69	-0.71	-0.53
5568	EBC	2018	s39	911.53	576.96	1,321.38	211.78	134.05	307.00	-0.32	-0.21
5568	EBC	2018	s40	270.39	207.41	341.60	45.90	35.21	57.99	-1.08	-0.99
5568	EBC	2018	s41	190.36	132.89	258.00	32.82	22.92	44.49	-1.17	-1.05
5568	EBC	2019	s42	241.47	159.65	339.94	45.97	30.39	64.72	-1.11	-0.99
5568	EBC	2019	s43	1,130.56	573.73	1,873.08	187.84	95.32	311.20	-0.06	-0.33
5568	EBC	2019	s44	1,356.97	736.17	2,164.46	206.34	111.94	329.12	0.20	-0.24
5568	EBC	2019	s45	2,350.45	1,395.74	3,549.91	424.69	252.19	641.41	1.37	0.78
5568	EBC	2019	s46	258.36	165.79	371.14	57.67	37.01	82.85	-1.09	-0.93
5568	EBC	2019	s47	1,663.29	922.00	2,619.66	278.70	154.49	438.94	0.56	0.10
5568	EBC	2019	s48	331.80	200.44	495.72	72.32	43.69	108.06	-1.01	-0.87
5568	EBC	2019	s49	721.86	436.33	1,078.09	157.16	95.00	234.71	-0.55	-0.47
5568	EBC	2019	s50	387.41	252.79	550.31	59.60	38.89	84.66	-0.94	-0.92
5568	EBC	2019	s51	488.40	293.97	731.37	90.57	54.51	135.63	-0.82	-0.78

ID	Tagging site	Year	Subset	Estimated 95%	Lower CI 95%	Upper CI 95%	Estimated 50%	Lower CI 50%	Upper CI 50%	Scale est. 95%	Scaled est. 50%
5568	EBC	2019	s52	2,379.73	1,469.18	3,506.31	518.55	320.14	764.04	1.41	1.22
5568	EBC	2019	s53	2,918.01	1,881.05	4,178.98	838.51	540.53	1,200.86	2.04	2.71
5568	EBC	2019	s54	1,730.42	1,105.75	2,492.71	272.01	173.82	391.84	0.64	0.07
5570	EBC	2017	s1	134.37	97.89	176.54	28.07	20.45	36.88	-0.85	-0.82
5570	EBC	2017	s2	255.99	191.57	329.60	52.78	39.50	67.95	-0.79	-0.77
5570	EBC	2017	s3	1,798.56	1,264.20	2,425.63	438.02	307.88	590.74	0.03	0.03
5570	EBC	2017	s4	631.31	453.55	838.00	137.02	98.44	181.88	-0.59	-0.60
5570	EBC	2017	s5	670.48	474.62	899.65	154.31	109.23	207.05	-0.57	-0.56
5570	EBC	2017	s6	1,407.21	1,026.55	1,846.98	310.97	226.85	408.16	-0.18	-0.24
5570	EBC	2017	s7	2,312.61	1,693.33	3,026.92	608.97	445.89	797.06	0.30	0.38
5570	EBC	2017	s8	2,306.96	1,635.56	3,092.01	589.41	417.88	789.99	0.30	0.34
5570	EBC	2017	s9	1,217.40	859.56	1,636.54	309.38	218.44	415.90	-0.28	-0.24
5570	EBC	2017	s10	1,138.71	812.32	1,519.36	228.99	163.35	305.54	-0.32	-0.41
5570	EBC	2017	s11	3,534.32	2,508.95	4,732.62	1,107.22	785.99	1,482.62	0.94	1.42
5570	EBC	2017	s12	1,676.79	1,202.45	2,228.77	504.43	361.74	670.49	-0.04	0.17
5570	EBC	2017	s13	1,536.62	1,111.61	2,029.35	303.87	219.83	401.31	-0.11	-0.25
5570	EBC	2017	s14	1,504.35	1,059.69	2,025.69	450.91	317.63	607.17	-0.13	0.06
5570	EBC	2017	s15	2,350.19	1,623.92	3,208.58	573.62	396.36	783.13	0.32	0.31
5570	EBC	2017	s16	529.87	398.69	679.42	135.85	102.22	174.18	-0.64	-0.60
5570	EBC	2018	s17	496.57	369.04	642.74	130.47	96.97	168.88	-0.66	-0.61
5570	EBC	2018	s18	2,618.85	1,418.99	4,180.26	594.68	322.22	949.24	0.46	0.35
5570	EBC	2018	s19	126.92	91.57	167.95	35.30	25.46	46.71	-0.86	-0.81
5570	EBC	2018	s20	39.99	30.50	50.75	8.80	6.71	11.17	-0.90	-0.86
5570	EBC	2018	s21	59.74	45.55	75.82	14.85	11.32	18.85	-0.89	-0.85
5570	EBC	2018	s22	40.63	31.93	50.35	7.87	6.18	9.75	-0.90	-0.87
5570	EBC	2018	s23	57.88	44.79	72.63	13.47	10.42	16.90	-0.89	-0.85
5570	EBC	2018	s24	81.67	62.70	103.11	22.62	17.37	28.56	-0.88	-0.83
5570	EBC	2018	s25	90.61	69.30	114.73	17.45	13.34	22.09	-0.88	-0.85
5570	EBC	2018	s26	2,615.37	1,195.75	4,581.04	654.59	299.28	1,146.56	0.46	0.48
5570	EBC	2018	s27	2,055.66	1,027.86	3,433.67	392.43	196.22	655.49	0.16	-0.07

ID	Tagging site	Year	Subset	Estimated 95%	Lower CI 95%	Upper CI 95%	Estimated 50%	Lower CI 50%	Upper CI 50%	Scale est. 95%	Scaled est. 50%
5570	EBC	2018	s28	1,654.93	1,181.90	2,206.33	345.92	247.05	461.18	-0.05	-0.16
5570	EBC	2018	s29	3,321.72	2,371.35	4,429.73	933.25	666.24	1,244.56	0.83	1.06
5570	EBC	2018	s30	1,005.53	687.44	1,383.15	263.93	180.44	363.05	-0.39	-0.33
5570	EBC	2018	s31	4,297.62	2,745.88	6,191.34	1,096.99	700.90	1,580.37	1.35	1.40
5570	EBC	2018	s32	3,586.92	2,598.26	4,732.49	776.98	562.82	1,025.13	0.97	0.73
5570	EBC	2018	s33	3,172.88	2,168.61	4,365.24	772.84	528.22	1,063.26	0.75	0.72
5570	EBC	2018	s34	2,018.25	1,480.08	2,638.57	418.18	306.68	546.72	0.14	-0.01
5570	EBC	2018	s35	2,681.82	1,962.44	3,511.80	683.10	499.86	894.51	0.49	0.54
5570	EBC	2018	s36	4,161.61	2,937.44	5,595.68	734.93	518.74	988.18	1.28	0.65
5570	EBC	2018	s37	4,490.48	2,454.93	7,130.45	965.99	528.10	1,533.90	1.45	1.13
5570	EBC	2018	s38	328.07	235.77	435.37	87.82	63.12	116.55	-0.75	-0.70
5570	EBC	2018	s39	246.68	176.60	328.30	67.69	48.46	90.08	-0.79	-0.74
5570	EBC	2018	s40	337.58	250.86	436.97	86.95	64.61	112.54	-0.75	-0.70
5570	EBC	2018	s41	157.30	115.84	205.01	33.87	24.94	44.14	-0.84	-0.81
5570	EBC	2019	s42	49.73	37.25	63.99	13.76	10.31	17.71	-0.90	-0.85
5570	EBC	2019	s43	1,032.62	583.79	1,607.35	148.90	84.18	231.78	-0.38	-0.57
5570	EBC	2019	s44	2,757.20	1,282.01	4,787.65	677.42	314.98	1,176.28	0.53	0.53
5570	EBC	2019	s45	1,957.72	552.99	4,234.12	371.16	104.84	802.75	0.11	-0.11
5570	EBC	2019	s46	831.11	130.77	2,165.59	187.04	29.43	487.36	-0.48	-0.49
5570	EBC	2019	s47	595.98	355.40	897.74	87.27	52.04	131.46	-0.61	-0.70
5570	EBC	2019	s48	114.66	86.87	146.26	24.96	18.91	31.84	-0.86	-0.83
5570	EBC	2019	s49	173.86	130.90	222.82	45.16	34.00	57.88	-0.83	-0.79
5570	EBC	2019	s50	258.39	162.48	376.19	58.18	36.58	84.70	-0.79	-0.76
5570	EBC	2019	s51	3,346.09	1,278.00	6,392.06	769.96	294.08	1,470.86	0.85	0.72
5570	EBC	2019	s52	8,549.49	3,684.12	15,427.60	2,007.25	864.96	3,622.09	3.60	3.29
5570	EBC	2019	s53	7,801.55	3,035.11	14,778.71	2,132.02	829.44	4,038.75	3.20	3.55
5570	EBC	2019	s54	111.69	83.13	144.41	20.55	15.29	26.57	-0.87	-0.84
5570	EBC	2019	s55	6,554.80	3,617.99	10,349.86	1,793.80	990.10	2,832.36	2.54	2.85
5570	EBC	2019	s56	1,164.52	845.41	1,533.93	320.68	232.81	422.41	-0.31	-0.22
5570	EBC	2019	s57	1,589.94	1,157.05	2,090.55	431.92	314.32	567.91	-0.08	0.02

ID	Tagging site	Year	Subset	Estimated 95%	Lower CI 95%	Upper CI 95%	Estimated 50%	Lower CI 50%	Upper CI 50%	Scale est. 95%	Scaled est. 50%
5573*	Barreiras	2018	s1	193.59	87.10	341.89	33.76	15.19	59.62	-	-
5574*	B. do Chico	2018	s1	156.57	96.88	230.36	43.13	26.69	63.45	-	-
6444	BDO	2021	s1	39.03	30.15	49.04	9.78	7.55	12.28	0.85	-0.17
6444	BDO	2021	s2	5.34	4.73	5.99	1.12	0.99	1.26	-0.64	-0.64
6444	BDO	2021	s3	6.43	5.65	7.26	1.31	1.15	1.48	-0.59	-0.63
6444	BDO	2021	s4	9.11	7.76	10.57	1.79	1.52	2.07	-0.47	-0.61
6444	BDO	2021	s5	7.22	6.34	8.16	1.13	0.99	1.28	-0.55	-0.64
6444	BDO	2021	s6	14.04	12.30	15.89	1.90	1.66	2.15	-0.25	-0.60
6444	BDO	2021	s7	1.37	0.10	4.23	30.34	2.26	93.85	-0.81	0.96
6444	BDO	2021	s8	45.15	35.91	55.43	6.10	4.85	7.49	1.11	-0.37
6444	BDO	2021	s10	1.70	1.49	1.93	17.50	15.33	19.82	-0.80	0.25
6444	BDO	2021	s11	2.98	2.46	3.56	54.95	45.26	65.57	-0.74	2.30
6444	BDO	2021	s12	4.44	3.89	5.02	61.70	54.08	69.82	-0.68	2.67
6444	BDO	2021	s13	17.47	15.39	19.68	1.67	1.47	1.88	-0.10	-0.61
6444	BDO	2021	s14	26.99	23.57	30.64	1.95	1.70	2.21	0.32	-0.60
6444	BDO	2021	s15	5.21	4.63	5.82	47.00	41.80	52.51	-0.64	1.87
6444	BDO	2021	s16	6.24	5.54	6.98	62.43	55.45	69.81	-0.60	2.71
6444	BDO	2021	s17	46.12	38.29	54.66	6.86	5.70	8.13	1.16	-0.33
6444	BDO	2021	s18	12.87	10.11	15.95	2.62	2.06	3.24	-0.30	-0.56
6444	BDO	2021	s19	9.62	7.72	11.73	1.77	1.42	2.16	-0.45	-0.61
6444	BDO	2021	s20	2.68	2.28	3.11	34.43	29.28	39.99	-0.75	1.18
6444	BDO	2021	s21	25.66	19.59	32.53	4.12	3.15	5.23	0.26	-0.48
6444	BDO	2021	s22	1.78	1.51	2.08	25.08	21.26	29.20	-0.79	0.67
6444	BDO	2022	s23	18.73	17.03	20.51	3.95	3.59	4.33	-0.05	-0.49
6444	BDO	2022	s24	1.25	1.03	1.48	20.35	16.86	24.17	-0.82	0.41
6444	BDO	2022	s25	2.84	2.27	3.48	43.57	34.84	53.26	-0.75	1.68
6444	BDO	2022	s26	27.58	24.27	31.10	4.21	3.70	4.75	0.34	-0.47
6444	BDO	2022	s27	2.62	2.14	3.15	37.87	30.88	45.56	-0.76	1.37
6444	BDO	2022	s28	14.75	13.39	16.18	3.19	2.90	3.50	-0.22	-0.53
6444	BDO	2022	s29	3.79	2.93	4.76	60.77	47.01	76.27	-0.70	2.62

ID	Tagging site	Year	Subset	Estimated 95%	Lower CI 95%	Upper CI 95%	Estimated 50%	Lower CI 50%	Upper CI 50%	Scale est. 95%	Scaled est. 50%
6444	BDO	2022	s30	21.53	17.88	25.52	4.09	3.40	4.85	0.08	-0.48
6444	BDO	2022	s31	12.89	10.61	15.40	2.72	2.23	3.24	-0.30	-0.56
6444	BDO	2022	s32	15.42	12.40	18.76	3.37	2.71	4.10	-0.19	-0.52
6444	BDO	2022	s33	14.07	11.81	16.52	2.43	2.04	2.85	-0.25	-0.57
6444	BDO	2022	s34	10.89	9.42	12.47	2.10	1.82	2.41	-0.39	-0.59
6444	BDO	2022	s35	16.05	13.65	18.63	3.18	2.70	3.69	-0.16	-0.53
6444	BDO	2022	s36	19.63	15.29	24.51	3.47	2.70	4.33	-0.01	-0.52
6444	BDO	2022	s37	23.00	18.68	27.76	4.59	3.73	5.54	0.14	-0.45
6444	BDO	2022	s38	24.03	20.69	27.61	4.03	3.47	4.63	0.19	-0.48
6444	BDO	2022	s39	35.70	27.59	44.83	7.56	5.84	9.49	0.70	-0.29
6444	BDO	2022	s40	147.28	112.74	186.36	13.52	10.35	17.11	5.60	0.04
6444	BDO	2022	s41	37.93	30.94	45.63	2.79	2.27	3.35	0.80	-0.55
6444	BDO	2022	s42	15.22	12.42	18.29	1.68	1.37	2.02	-0.20	-0.61
6444	BDO	2022	s43	34.99	29.58	40.85	4.69	3.97	5.48	0.67	-0.45
6444	BDO	2022	s44	46.20	37.70	55.55	4.04	3.30	4.86	1.16	-0.48
6444	BDO	2022	s45	18.41	14.78	22.43	2.55	2.05	3.11	-0.06	-0.57
6444	BDO	2022	s46	27.53	22.29	33.31	3.67	2.97	4.44	0.34	-0.50
6444	BDO	2023	s47	10.07	8.49	11.79	1.80	1.51	2.10	-0.43	-0.61
6444	BDO	2023	s48	21.59	20.43	22.78	1.33	1.26	1.40	0.08	-0.63
6444	BDO	2023	s49	42.16	37.17	47.45	6.03	5.31	6.79	0.98	-0.37
6444	BDO	2023	s50	12.31	9.62	15.33	1.87	1.46	2.32	-0.33	-0.60
9015	BDO	2021	s1	94.11	74.20	116.35	17.40	13.72	21.52	1.15	1.15
9015	BDO	2021	s2	9.43	8.74	10.16	1.57	1.45	1.69	-0.61	-0.57
9024*	B. do Chico	2021	s1	120.08	87.60	157.60	23.32	17.01	30.60	-	-
9026	Barreiras	2022	s1	87.67	65.77	112.66	24.23	18.18	31.14	-	-
9250	Barreiras	2022	s1	376.08	252.92	523.30	77.40	52.05	107.70	0.71	0.71
9250*	Barreiras	2022	s2	76.37	50.67	107.25	14.98	9.94	21.04	-0.71	-0.71
9252*	Barreiras	2022	s1	142.05	46.25	290.64	33.26	10.83	68.05	-	-
9025	B. do Chico	2021	s1	131.85	97.26	171.62	27.47	20.27	35.76	-0.54	-0.42
9025	B. do Chico	2021	s2	147.84	110.33	190.75	36.04	26.90	46.50	-0.48	-0.27

ID	Tagging site	Year	Subset	Estimated 95%	Lower CI 95%	Upper CI 95%	Estimated 50%	Lower CI 50%	Upper CI 50%	Scale est. 95%	Scaled est. 50%
9025	B. do Chico	2021	s3	114.90	85.78	148.20	20.49	15.30	26.43	-0.61	-0.55
9025	B. do Chico	2021	s4	101.28	75.56	130.71	16.94	12.64	21.86	-0.67	-0.61
9025	B. do Chico	2021	s5	133.82	101.28	170.81	28.34	21.45	36.18	-0.54	-0.41
9025	B. do Chico	2021	s6	156.64	117.78	200.94	30.18	22.70	38.72	-0.44	-0.38
9025	B. do Chico	2021	s7	123.71	93.61	157.94	20.76	15.71	26.50	-0.58	-0.55
9025	B. do Chico	2021	s8	150.65	113.38	193.13	35.77	26.92	45.86	-0.47	-0.27
9025	B. do Chico	2021	s9	114.13	85.37	147.00	19.79	14.80	25.48	-0.62	-0.56
9025	B. do Chico	2021	s10	169.97	128.16	217.59	29.14	21.97	37.31	-0.39	-0.39
9025	B. do Chico	2021	s11	94.21	70.34	121.51	16.68	12.46	21.52	-0.70	-0.62
9025	B. do Chico	2021	s12	80.35	59.11	104.81	18.33	13.48	23.91	-0.75	-0.59
9025	B. do Chico	2022	s13	119.95	88.87	155.62	20.47	15.17	26.56	-0.59	-0.55
9025	B. do Chico	2022	s14	108.13	80.79	139.40	14.18	10.59	18.27	-0.64	-0.66
9025	B. do Chico	2022	s15	128.18	99.99	159.83	15.07	11.76	18.79	-0.56	-0.65
9025	B. do Chico	2022	s16	284.62	203.37	379.30	38.51	27.52	51.33	0.08	-0.22
9025	B. do Chico	2022	s17	223.58	163.03	293.54	26.51	19.33	34.81	-0.17	-0.44
9025	B. do Chico	2022	s18	464.88	335.30	615.29	79.44	57.30	105.14	0.82	0.52
9025	B. do Chico	2022	s19	291.77	204.56	394.21	49.22	34.51	66.50	0.11	-0.03
9025	B. do Chico	2022	s20	180.90	138.21	229.24	30.16	23.04	38.22	-0.34	-0.38
9025	B. do Chico	2022	s21	237.34	178.90	303.93	45.79	34.52	58.64	-0.11	-0.09
9025	B. do Chico	2022	s22	872.84	626.91	1,158.83	219.53	157.67	291.46	2.48	3.05
9025	B. do Chico	2022	s23	301.38	224.55	389.34	77.25	57.56	99.80	0.15	0.48
9025	B. do Chico	2022	s24	303.73	225.86	392.96	45.72	34.00	59.15	0.16	-0.09
9025	B. do Chico	2022	s25	397.24	290.75	520.10	59.02	43.20	77.27	0.54	0.15
9025	B. do Chico	2022	s26	835.29	570.13	1,150.29	213.00	145.39	293.33	2.33	2.93
9025	B. do Chico	2022	s27	525.45	384.15	688.53	92.27	67.46	120.90	1.06	0.75
9025	B. do Chico	2022	s28	558.66	393.57	752.21	89.03	62.72	119.88	1.20	0.69
9025	B. do Chico	2022	s34	606.44	336.86	953.96	161.22	89.56	253.61	1.39	2.00
9025	B. do Chico	2022	s35	67.04	51.57	84.50	15.44	11.88	19.46	-0.81	-0.64
9025	B. do Chico	2022	s36	114.84	87.71	145.58	19.94	15.23	25.28	-0.61	-0.56
9025	B. do Chico	2023	s37	134.91	103.18	170.81	22.63	17.31	28.65	-0.53	-0.51

ID	Tagging site	Year	Subset	Estimated 95%	Lower CI 95%	Upper CI 95%	Estimated 50%	Lower CI 50%	Upper CI 50%	Scale est. 95%	Scaled est. 50%
9025	B. do Chico	2023	s38	98.08	74.12	125.34	16.04	12.12	20.50	-0.68	-0.63
9025	B. do Chico	2023	s39	511.70	335.98	723.81	95.98	63.02	135.76	1.01	0.81
9025	B. do Chico	2023	s40	48.16	36.47	61.46	5.69	4.31	7.26	-0.89	-0.82
9025	B. do Chico	2023	s41	12.66	9.68	16.02	1.67	1.28	2.11	-1.03	-0.89
9025	B. do Chico	2023	s42	51.10	34.12	71.45	6.20	4.14	8.67	-0.87	-0.81
9025	B. do Chico	2023	s43	31.15	22.89	40.67	3.83	2.82	5.00	-0.95	-0.85
9025	B. do Chico	2023	s44	151.49	104.66	206.84	17.88	12.36	24.42	-0.46	-0.60
9025	B. do Chico	2023	s45	833.69	577.54	1,136.12	142.66	98.83	194.41	2.32	1.66
9025	B. do Chico	2023	s46	855.17	585.85	1,174.63	163.83	112.24	225.04	2.41	2.04

SUPPLEMENTARY MATERIAL 3 Details on home range and core area estimation.

Using the ctmm framework (Calabrese et al., 2016), we compared the fit of movement models (Independent Identically Distributed (IID), Ornstein-Uhlenbeck (OU) and Ornstein-Uhlenbeck Foraging (OUF)) to our data using the autocorrelation estimation method. Once the range residency was determined – required by the ctmm package to calculate the AKDE ranges (Isted et al., 2023) –, the best model was selected (via Akaike Information Criterion – AIC) and applied to fit the function of the AKDE to estimate ranges' size (Calabrese et al., 2016). We calculated the home ranges using 95% AKDE (corresponding to the individual's mobility potential in the total area); and the core areas, using 50% AKDE (corresponding to the areas that the animal uses most frequently; Supplementary Table 3) (Fleming et al., 2015; Redpath et al., 2023).

Due to the large variation of home ranges' and core areas' estimates among individuals, instead of using the absolute values of home range and core areas estimates in the model analysis, we scaled them using "scale" function in base R software (R Core Team, 2023; the centralization argument used for the variables was the average of each individuals' estimates; Supplementary Table 4). The scaling procedure allowed fitting of models with data from multiple macaws simultaneously – comparatively observing the variation in fortnightly estimates of ranges over time to evaluate the influence of the predictor variables when adjusting the models.

References

REDPATH, S.H.A., MARKS, N.J., MENZIES, F.D., O'HAGAN, M.J.H., WILSON, R.P., SMITH, S. ET AL. (2023) Impact of test, vaccinate and remove protocol on home ranges and nightly movements of badgers in a medium density population. *Scientific Reports*, 13, 2592.

SUPPLEMENTARY TABLE 4 Updated summary with identification of the tagged macaws for which we retrieved movement data, the tagging site (RASO = breeding sites in *Raso da Catarina* region, BDO = release area in *Boqueirão da Onça* region), the tagging date (year-month-day format), dates of the first and the last data download in the field, the total number of days ("Duration") for which there is movement data recorded for each macaw, and the total number of points recorded for each individual.

ID	**Tagging site**	**Tagging date**	**1st download**	**Last download**	**Duration (days)**	**Nº of points**
5568	RASO	2017-04-24	2017-05-03	2019-07-26	815	73,811
5570	RASO	2017-04-26	2017-05-03	2019-09-07	858	55,308
5573	RASO	2018-06-15	2018-06-26	2018-06-30	5	419
5574	RASO	2018-06-25	2018-07-07	2018-07-12	6	178
9015	BDO	2021-02-09	2021-02-09	2021-03-22	42	3,194
6444	BDO	2021-02-09	2021-02-09	2024-10-20	1,346	668,473
9024	RASO	2021-06-29	2021-07-09	2021-07-21	13	1,154
9025	RASO	2021-06-29	2021-07-09	2023-05-29	690	34,279
9026	RASO	2022-04-19	2022-04-29	2022-05-20	22	1,893
9250	RASO	2022-04-25	2022-04-30	2022-05-20	21	2,356
9252	RASO	2022-06-17	2022-06-27	2022-06-30	4	696

SUPPLEMENTARY MATERIAL 4 Details on environmental predictors and data processing, indicating how each variable was prepared for the home range and core area size temporal variation analysis.

We evaluated intra-annual and interannual variation in home range and core area size of tagged juvenile Lear's macaws using linear models (bbmle R package; Rencher & Schaalje, 2008; R Core Team, 2023). We investigated whether the predictor variables "tagging site" (communal roost site where the individual was born or released and tagged), "season", "ordinal date", "accumulated rainfall over the last six months", "accumulated rainfall over the last twelve months", "NDVI data relative to the real coordinates", and "NDVI data relative to the random coordinates" influenced the temporal variation in size of the ranges estimated for the macaws.

For seasonal evaluation, considering that most of rainfall in Caatinga is concentrated in few consecutive months, and the rainy season is centered upon March, April and May, we considered the months from January to May as the "wet season", and the "dry season", from June to December (Tabarelli et al., 2003; da Silva, 2004; Silva et al., 2017). The "ordinal date" was also incorporated into the analysis as a predictor variable representing the seasonality throughout the year. In this analysis, the reference date for start counting the ordinal days (i.e., the ordinal date number 1) of a given subset of movement data always corresponded to January 1st of the year of that subset. Therefore, the count of consecutive days was restarted every new year – and the lower the count of the ordinal days, the closer the movement data subset was to the beginning of that year.

We also assessed if the licuri palm (*S. coronata*) fruit availability was related to temporal variation of the size of estimated ranges. The licuri palm fruit availability (therefore, the environmental productivity and resource availability) was inferred from climate remote sensing data (rainfall precipitation) and vegetation data (primary productivity index, more specifically, the Normalized Difference Vegetation Index – NDVI). The regional vegetation dynamics in semi-arid is strongly correlated with rainfall, and the NDVI, by measuring vegetation productivity/availability, is highly correlated to precipitation in the Caatinga – with the seasonal NDVI oscillation being related to the seasonal distribution of dry and wet periods, and also fluctuating according to the year rainfall (Pettorelli et al., 2005; Schucknecht et al., 2013; Barbosa et al., 2015; Silva et al., 2017).

Historical daily rainfall data series were extracted from meteorological stations within species' occurrence area from the Hidroweb platform (v3.2.7), managed by the Brazilian National Water and Basic Sanitation Agency (ANA). Aiming to investigate whether the movement of the macaws – and, therefore, the size variation of their ranges – would respond to changes in licuri palm fruit availability, the precipitation data was grouped into time series of accumulated rainfall (of both six and twelve months prior to start dates of each fortnightly movement data subset; supporting information in Supplementary Table 5). The temporal scales of rainfall were selected based on reproductive phenology of licuri palm and, therefore, on the estimated time for fruit development, ripening and availability. The *S. coronata* inflorescence requires five to ten months to fully develop. After this period, and after the time needed to mature the male and female flowers (ca. 40 days), the palm requires approximately another two months for fruits to ripen (Barbosa et al., 2021).

The NDVI was obtained from Movebank Environmental Data Automated Track Annotation System (Env-DATA) for the animals' tracking data (Dodge et al., 2013; Kays et al., 2022). We used NASA product MODIS Land Vegetation Indices MOD13Q1 V6.1 with spatial resolution/granularity = 250 m, and temporal resolution/granularity = 16-day period. To incorporate the NDVI data into the linear models, the median of the NDVI values was calculated for each fortnightly range estimated (Supplementary Table 5).

Through the inverse distance weighted interpolation method, recommended in case of observation-driven variables, such as MODIS products (Dodge et al., 2013), Movebank annotated the tracking data by calculating estimated values of the variable for the location and time of each animal location – using values provided by the NDVI dataset for specific locations and times (Dodge et al., 2013; Kays et al., 2022). Considering that NDVI varies over time, each location was associated with the specific NDVI value corresponding to that location at the closest date (Viana et al., 2018).

Furthermore, aiming to understand whether the general productivity of the landscape would also influence on macaws' range sizes temporal variation, we included in the analysis, as another predictor variable, the median of NDVI values calculated for randomized geographic coordinates in the landscape – located within the bounding boxes of the estimated individual AKDE ranges, calculated in QGIS software (QGIS Development Team, 2023). The number of randomized geographic coordinates generated was the same as the real coordinates recorded for each individual, during its entire period of monitoring. The random NDVI data worked as a proxy for the availability of licuri in the environment. The random coordinates were also linked to the NDVI dataset by the Env-DATA (Dodge et al., 2013; Kays et al., 2022).

References

BARBOSA, C.M., MAIA, A.C.D., MARTEL, C., REGUEIRA, J.C.S., NAVARRO, D.M. DO A.F., RAGUSO, R.A., ET AL. (2021) Reproductive biology of *Syagrus coronata* (*Arecaceae*): sex-biased insect visitation and the unusual case of scent emission by peduncular bracts. *Plant Biology*, 23, 100–110.

BARBOSA, H.A., LAKSHMI KUMAR, T.V., SILVA, L.R.M. (2015) Recent trends in vegetation dynamics in the South America and their relationship to rainfall. *Natural Hazards*, 77, 883–899.

DODGE, S., BOHRER, G., WEINZIERL, R., DAVIDSON, S.C., KAYS, R., DOUGLAS, D., ET AL. (2013) The environmental-data automated track annotation (Env-DATA) system: linking animal tracks with environmental data. *Movement Ecology*, 1, 3.

SCHUCKNECHT, A., ERASMI, S., NIEMEYER, I. & MATSCHULLAT, J. (2013) Assessing vegetation variability and trends in north-eastern Brazil using AVHRR and MODIS NDVI time series. *European Journal of Remote Sensing*, 46, 40–59.

DA SILVA, V. DE P.R. (2004) On climate variability in Northeast of Brazil. *Journal of Arid Environments*, 58, 575–596.

TABARELLI, M., VICENTE, A. & BARBOSA, D. C. A. (2003) Variation of seed dispersal spectrum of woody plants across a rainfall gradient in north-eastern Brazil. *Journal of Arid Environments*, 53, 197–210.

SUPPLEMENTARY TABLE 5 Rainfall data and Normalized Difference Vegetation Index (NDVI) data for each fortnightly subset of macaw movement data, with identification of the individual ("ID"), the fortnightly subset of macaw movement data ("Subset"), the month, season and ordinal date of the respective fortnightly subset, the identification of the rainfall station from which the rainfall data were extracted, the accumulated rainfall (in millimeters) for six ("Accum. rainfall 6") and 12 months ("Accum. rainfall 12"), and the median of the NDVI data associated with the real coordinates ("Real NDVI median") recorded for the macaws and the median of the NDVI data associated with the generated random coordinates ("Random NDVI median").

ID	Subset	Month	Season	Ordinal date	Rainfall station	Accum. rainfall 6	Accum. rainfall 12	Real NDVI median	Random NDVI median
5568	s1	may	wet	122	Alto Redondo	114.4	193.4	0.37	0.41
5568	s2	may	wet	137	Alto Redondo	113.6	171.9	0.39	0.47
5568	s3	june	dry	152	Alto Redondo	149.3	201.6	0.42	0.49
5568	s4	june	dry	167	Alto Redondo	133.3	200.7	0.35	0.44
5568	s5	july	dry	182	Alto Redondo	144.9	203.5	0.47	0.50
5568	s6	july	dry	197	Alto Redondo	142.7	208.7	0.47	0.53
5568	s7	august	dry	212	Alto Redondo	148.1	211.9	0.40	0.45
5568	s8	august	dry	227	Alto Redondo	148.1	211.2	0.44	0.37
5568	s9	september	dry	242	Alto Redondo	148.1	208.9	0.42	0.40
5568	s10	september	dry	257	Alto Redondo	170.8	237.2	0.56	0.44
5568	s11	october	dry	272	Alto Redondo	121.7	238.7	0.52	0.63
5568	s12	october	dry	287	Alto Redondo	113.7	226.1	0.49	0.52
5568	s13	november	dry	302	Alto Redondo	111.7	226.1	0.38	0.37
5568	s14	november	dry	317	Alto Redondo	121.6	235.2	0.36	0.38
5568	s15	december	dry	332	Alto Redondo	85.9	235.2	0.33	0.35
5568	s16	december	dry	347	Alto Redondo	95	257.6	0.26	0.32
5568	s17	january	wet	362	Alto Redondo	83.4	228.3	0.30	0.36
5568	s18	january	wet	12	Alto Redondo	84.8	227.5	0.30	0.35
5568	s19	february	wet	27	Alto Redondo	85.7	233.8	0.26	0.33
5568	s20	february	wet	42	Alto Redondo	108.2	256.3	0.29	0.35
5568	s21	march	wet	57	Alto Redondo	179.2	327.3	0.36	0.45
5568	s22	march	wet	72	Alto Redondo	166.3	345.8	0.39	0.43
5568	s23	april	wet	87	Alto Redondo	165.6	339.5	0.37	0.42
5568	s24	april	wet	102	Alto Redondo	229.5	354.6	0.30	0.41

ID	Subset	Month	Season	Ordinal date	Rainfall station	Accum. rainfall 6	Accum. rainfall 12	Real NDVI median	Random NDVI median
5568	s25	may	wet	117	Alto Redondo	237.8	351.5	0.41	0.40
5568	s26	may	wet	132	Alto Redondo	254.6	63.8	0.36	0.47
5568	s27	june	dry	147	Alto Redondo	254.6	341.1	0.34	0.47
5568	s28	june	dry	162	Alto Redondo	244.4	349.6	0.34	0.45
5568	s29	july	dry	177	Alto Redondo	244.4	329.1	0.39	0.43
5568	s30	july	dry	192	Alto Redondo	235.5	321.2	0.42	0.39
5568	s31	august	dry	207	Alto Redondo	228.9	314.6	0.34	0.33
5568	s32	august	dry	222	Alto Redondo	206.4	314.6	0.31	0.33
5568	s33	september	dry	237	Alto Redondo	140.3	319.5	0.34	0.33
5568	s34	september	dry	252	Alto Redondo	121.8	301.5	0.30	0.31
5568	s35	october	dry	267	Alto Redondo	119.4	285	0.30	0.28
5568	s36	october	dry	282	Alto Redondo	52.1	281.6	0.28	0.27
5568	s37	november	dry	297	Alto Redondo	43.8	281.6	0.25	0.25
5568	s38	november	dry	312	Alto Redondo	17.1	281.6	0.25	0.24
5568	s39	december	dry	327	Alto Redondo	17.1	271.7	0.29	0.33
5568	s40	december	dry	342	Alto Redondo	148.8	415.6	0.41	0.48
5568	s41	december	dry	357	Alto Redondo	149	393.4	0.43	0.54
5568	s42	january	wet	7	Alto Redondo	149	384.5	0.36	0.47
5568	s43	january	wet	22	Alto Redondo	149	377.9	0.33	0.47
5568	s44	february	wet	37	Alto Redondo	154.2	360.6	0.34	0.49
5568	s45	march	wet	52	Alto Redondo	149.3	331.1	0.33	0.47
5568	s46	march	wet	67	Alto Redondo	159	282.8	0.31	0.40
5568	s47	march	wet	82	Alto Redondo	204.4	326.2	0.39	0.56
5568	s48	april	wet	97	Alto Redondo	332.6	384.7	0.45	0.60
5568	s49	april	wet	112	Alto Redondo	332.6	376.4	0.41	0.53
5568	s50	may	wet	127	Alto Redondo	359.3	376.4	0.41	0.49
5568	s51	may	wet	142	Alto Redondo	382.3	399.4	0.43	0.49
5568	s52	june	dry	157	Alto Redondo	241.9	390.7	0.50	0.58
5568	s53	june	dry	172	Alto Redondo	285.9	434.9	0.61	0.60
5568	s54	july	dry	187	Alto Redondo	287.5	436.5	0.40	0.60

ID	Subset	Month	Season	Ordinal date	Rainfall station	Accum. rainfall 6	Accum. rainfall 12	Real NDVI median	Random NDVI median
5570	s1	may	wet	122	Alto Redondo	114.4	193.4	0.33	0.41
5570	s2	may	wet	137	Alto Redondo	113.6	171.9	0.40	0.46
5570	s3	june	dry	152	Alto Redondo	149.3	201.6	0.46	0.48
5570	s4	june	dry	167	Alto Redondo	133.3	200.7	0.38	0.43
5570	s5	july	dry	182	Alto Redondo	144.9	203.5	0.50	0.48
5570	s6	july	dry	197	Alto Redondo	142.7	208.7	0.50	0.50
5570	s7	august	dry	212	Alto Redondo	148.1	211.9	0.41	0.46
5570	s8	august	dry	227	Alto Redondo	148.1	211.2	0.40	0.35
5570	s9	september	dry	242	Alto Redondo	148.1	208.9	0.42	0.35
5570	s10	september	dry	257	Alto Redondo	170.8	237.2	0.51	0.39
5570	s11	october	dry	272	Alto Redondo	121.7	238.7	0.59	0.47
5570	s12	october	dry	287	Alto Redondo	113.7	226.1	0.46	0.40
5570	s13	november	dry	302	Alto Redondo	111.7	226.1	0.38	0.36
5570	s14	november	dry	317	Alto Redondo	121.6	235.2	0.37	0.34
5570	s15	december	dry	332	Alto Redondo	85.9	235.2	0.34	0.32
5570	s16	december	dry	347	Alto Redondo	95	257.6	0.33	0.31
5570	s17	january	wet	362	Alto Redondo	83.4	228.3	0.40	0.34
5570	s18	january	wet	12	Alto Redondo	84.8	227.5	0.35	0.34
5570	s19	february	wet	27	Alto Redondo	85.7	233.8	0.29	0.31
5570	s20	february	wet	42	Alto Redondo	108.2	256.3	0.29	0.33
5570	s21	march	wet	57	Alto Redondo	179.2	327.3	0.33	0.34
5570	s22	march	wet	72	Alto Redondo	166.3	345.8	0.39	0.38
5570	s23	april	wet	87	Alto Redondo	165.6	339.5	0.45	0.42
5570	s24	april	wet	102	Alto Redondo	229.5	354.6	0.39	0.40
5570	s25	may	wet	117	Alto Redondo	237.8	351.5	0.42	0.43
5570	s26	may	wet	132	Alto Redondo	254.6	63.8	0.45	0.47
5570	s27	june	dry	147	Alto Redondo	254.6	341.1	0.44	0.47
5570	s28	june	dry	162	Alto Redondo	244.4	349.6	0.39	0.46
5570	s29	july	dry	177	Alto Redondo	244.4	329.1	0.44	0.45
5570	s30	july	dry	192	Alto Redondo	235.5	321.2	0.43	0.38

ID	Subset	Month	Season	Ordinal date	Rainfall station	Accum. rainfall 6	Accum. rainfall 12	Real NDVI median	Random NDVI median
5570	s31	august	dry	207	Alto Redondo	228.9	314.6	0.36	0.34
5570	s32	august	dry	222	Alto Redondo	206.4	314.6	0.33	0.31
5570	s33	september	dry	237	Alto Redondo	140.3	319.5	0.30	0.29
5570	s34	september	dry	252	Alto Redondo	121.8	301.5	0.29	0.28
5570	s35	october	dry	267	Alto Redondo	119.4	285	0.27	0.26
5570	s36	october	dry	282	Alto Redondo	52.1	281.6	0.26	0.26
5570	s37	november	dry	297	Alto Redondo	43.8	281.6	0.26	0.26
5570	s38	november	dry	312	Alto Redondo	17.1	281.6	0.26	0.23
5570	s39	december	dry	327	Alto Redondo	17.1	271.7	0.29	0.32
5570	s40	december	dry	342	Alto Redondo	148.8	415.6	0.40	0.47
5570	s41	december	dry	357	Alto Redondo	149	393.4	0.39	0.48
5570	s42	january	wet	7	Alto Redondo	149	384.5	0.33	0.42
5570	s43	january	wet	22	Alto Redondo	149	377.9	0.29	0.44
5570	s44	february	wet	37	Alto Redondo	154.2	360.6	0.34	0.45
5570	s45	march	wet	52	Alto Redondo	149.3	331.1	0.30	0.49
5570	s46	march	wet	67	Alto Redondo	159	282.8	0.29	0.46
5570	s47	march	wet	82	Alto Redondo	204.4	326.2	0.36	0.56
5570	s48	april	wet	97	Alto Redondo	332.6	384.7	0.48	0.53
5570	s49	april	wet	112	Alto Redondo	332.6	376.4	0.47	0.45
5570	s50	may	wet	127	Alto Redondo	359.3	376.4	0.39	0.44
5570	s51	may	wet	142	Alto Redondo	382.3	399.4	0.53	0.55
5570	s52	june	dry	157	Alto Redondo	241.9	390.7	0.58	0.57
5570	s53	june	dry	172	Alto Redondo	285.9	434.9	0.63	0.64
5570	s54	july	dry	187	Alto Redondo	287.5	436.5	0.77	0.77
5570	s55	july	dry	202	Alto Redondo	318.6	467.6	0.73	0.65
5570	s56	august	dry	217	Alto Redondo	313.4	467.6	0.63	0.50
5570	s57	august	dry	232	Alto Redondo	323.3	477.5	0.52	0.47
6444	s1	february	wet	39	Limoeiro	262.7	752.4	0.60	0.58
6444	s2	march	wet	54	Limoeiro	325.6	815.3	0.57	0.57
6444	s3	march	wet	69	Limoeiro	329	664.7	0.49	0.50

ID	Subset	Month	Season	Ordinal date	Rainfall station	Accum. rainfall 6	Accum. rainfall 12	Real NDVI median	Random NDVI median
6444	s4	april	wet	84	Limoeiro	335.1	599.9	0.53	0.53
6444	s5	april	wet	99	Limoeiro	344.5	535.9	0.50	0.50
6444	s6	may	wet	114	Limoeiro	400.8	405.9	0.49	0.51
6444	s7	may	wet	129	Limoeiro	287.8	408.4	0.50	0.61
6444	s8	june	dry	144	Limoeiro	225.8	408.4	0.52	0.53
6444	s10	july	dry	174	Limoeiro	225.8	403.3	0.46	0.53
6444	s11	july	dry	189	Limoeiro	204.8	403.3	0.40	0.49
6444	s12	july	dry	204	Limoeiro	175.8	403.3	0.37	0.47
6444	s13	august	dry	219	Limoeiro	140.6	403.3	0.33	0.51
6444	s14	august	dry	234	Limoeiro	77.7	403.3	0.31	0.46
6444	s15	september	dry	249	Limoeiro	83.3	412.3	0.30	0.45
6444	s16	september	dry	264	Limoeiro	77.2	412.3	0.28	0.40
6444	s17	october	dry	279	Limoeiro	67.8	412.3	0.29	0.40
6444	s18	october	dry	294	Limoeiro	11.5	412.3	0.37	0.42
6444	s19	november	dry	309	Limoeiro	91	378.8	0.53	0.58
6444	s20	november	dry	324	Limoeiro	145.4	385.2	0.62	0.67
6444	s21	december	dry	339	Limoeiro	209.4	435.2	0.52	0.59
6444	s22	december	dry	354	Limoeiro	257.4	483.2	0.60	0.70
6444	s23	january	wet	4	Limoeiro	377.2	582	0.65	0.65
6444	s24	january	wet	19	Limoeiro	399.2	575	0.64	0.73
6444	s25	february	wet	34	Limoeiro	421.2	569.8	0.52	0.72
6444	s26	february	wet	49	Limoeiro	429.2	516.9	0.51	0.67
6444	s27	march	wet	64	Limoeiro	448.7	535.4	0.55	0.70
6444	s28	march	wet	79	Limoeiro	489.7	573	0.54	0.56
6444	s29	april	wet	94	Limoeiro	489.7	557.5	0.59	0.66
6444	s30	april	wet	109	Limoeiro	526.2	594	0.67	0.66
6444	s31	may	wet	124	Limoeiro	444.2	535.2	0.57	0.63
6444	s32	may	wet	139	Limoeiro	409.2	554.6	0.50	0.60
6444	s33	june	dry	154	Limoeiro	345.2	554.6	0.48	0.59
6444	s34	june	dry	169	Limoeiro	297.2	554.6	0.55	0.59

ID	Subset	Month	Season	Ordinal date	Rainfall station	Accum. rainfall 6	Accum. rainfall 12	Real NDVI median	Random NDVI median
6444	s35	july	dry	184	Limoeiro	177.4	554.6	0.57	0.60
6444	s36	july	dry	199	Limoeiro	155.4	554.6	0.47	0.58
6444	s37	august	dry	214	Limoeiro	133.4	554.6	0.39	0.52
6444	s38	august	dry	229	Limoeiro	125.4	554.6	0.40	0.48
6444	s39	september	dry	244	Limoeiro	96.9	554.6	0.39	0.46
6444	s40	september	dry	259	Limoeiro	55.9	545.6	0.39	0.33
6444	s41	october	dry	274	Limoeiro	62.4	552.1	0.35	0.50
6444	s42	october	dry	289	Limoeiro	25.9	552.1	0.34	0.39
6444	s43	november	dry	304	Limoeiro	55.9	582.1	0.43	0.48
6444	s44	november	dry	319	Limoeiro	151.8	561	0.53	0.57
6444	s45	december	dry	334	Limoeiro	207.8	564	0.60	0.68
6444	s46	december	dry	349	Limoeiro	272.8	570	0.60	0.75
6444	s47	january	wet	364	Limoeiro	359.1	536.5	0.70	0.75
6444	s48	january	wet	14	Limoeiro	374.1	544	0.64	0.72
6444	s49	february	wet	29	Limoeiro	397.6	531	0.69	0.74
6444	s50	february	wet	44	Limoeiro	397.6	531	0.57	0.70
9025	s1	july	dry	189	Quixaba	204.8	350.6	0.48	0.49
9025	s2	july	dry	204	Quixaba	209.8	353.3	0.48	0.47
9025	s3	august	dry	219	Quixaba	194.6	362.5	0.48	0.46
9025	s4	august	dry	234	Quixaba	197.2	361.1	0.40	0.39
9025	s5	september	dry	249	Quixaba	194	358.9	0.33	0.33
9025	s6	september	dry	264	Quixaba	194	358.9	0.32	0.32
9025	s7	october	dry	279	Quixaba	170.1	364	0.32	0.32
9025	s8	october	dry	294	Quixaba	161.8	364	0.31	0.32
9025	s9	november	dry	309	Quixaba	182	294	0.32	0.34
9025	s10	november	dry	324	Quixaba	149.9	287.6	0.33	0.37
9025	s11	december	dry	339	Quixaba	139.1	297	0.41	0.46
9025	s12	december	dry	354	Quixaba	133.6	297.5	0.48	0.51
9025	s13	january	wet	4	Quixaba	138.8	343.6	0.51	0.54
9025	s14	january	wet	19	Quixaba	198.9	408.7	0.60	0.61

ID	Subset	Month	Season	Ordinal date	Rainfall station	Accum. rainfall 6	Accum. rainfall 12	Real NDVI median	Random NDVI median
9025	s15	february	wet	34	Quixaba	261.5	456.1	0.63	0.63
9025	s16	february	wet	49	Quixaba	302.8	500.7	0.63	0.62
9025	s17	march	wet	64	Quixaba	400.6	594.6	0.65	0.61
9025	s18	march	wet	79	Quixaba	400.6	594.6	0.53	0.55
9025	s19	april	wet	94	Quixaba	399.4	576.3	0.48	0.54
9025	s20	april	wet	109	Quixaba	405.6	574.2	0.49	0.56
9025	s21	may	wet	124	Quixaba	376.9	559.7	0.50	0.58
9025	s22	may	wet	139	Quixaba	379.1	530.1	0.51	0.59
9025	s23	june	dry	154	Quixaba	452.5	605.8	0.60	0.63
9025	s24	june	dry	169	Quixaba	485.3	623.2	0.56	0.63
9025	s25	july	dry	184	Quixaba	482.5	634.6	0.59	0.57
9025	s26	july	dry	199	Quixaba	457.5	657.5	0.58	0.56
9025	s27	august	dry	214	Quixaba	398.6	660.6	0.60	0.54
9025	s28	august	dry	229	Quixaba	384.3	687.8	0.44	0.49
9025	s34	november	dry	319	Quixaba	361.8	740.9	0.38	0.54
9025	s35	december	dry	334	Quixaba	320.7	782.1	0.59	0.65
9025	s36	december	dry	349	Quixaba	325.2	811	0.65	0.72
9025	s37	january	wet	364	Quixaba	374.5	857	0.61	0.72
9025	s38	january	wet	14	Quixaba	338.4	795.9	0.55	0.65
9025	s39	february	wet	29	Quixaba	319.5	718.1	0.48	0.59
9025	s40	february	wet	44	Quixaba	290.5	674.8	0.50	0.64
9025	s41	march	wet	59	Quixaba	289	604.7	0.45	0.58
9025	s42	march	wet	74	Quixaba	284.9	576.3	0.51	0.57
9025	s43	april	wet	89	Quixaba	437.5	725	0.55	0.63
9025	s44	april	wet	104	Quixaba	457.2	744.7	0.57	0.60
9025	s45	may	wet	119	Quixaba	457.2	727.7	0.61	0.60
9025	s46	may	wet	134	Quixaba	365.3	728.8	0.58	0.66

SUPPLEMENTARY TABLE 6 Candidate models set for the home ranges and the respective predictor variables showing performance of the top model relative to others in the model set. The models are ordered from the lowest to the highest delta AIC value (dAIC, i.e., calculated difference between AIC value of the observed model and the candidate model with the lowest AIC). The simbol '*' in the column "Model and predictor variables" indicates interaction between the two variables tested in respective model.

Model and predictor variables (95% kernel)	**AIC**	**dAIC**	**Adjusted R^2**
season + tagging site	568.7478	0.0	0.02256
season * tagging site	568.8816	0.1	0.03135
real coordinates median NDVI	569.6104	0.9	0.008693
accumulated rainfall 12 months	570.1034	1.4	0.006259
null	570.3730	1.6	
accumulated rainfall 6 months	571.4172	2.7	-0.0002577
random coordinates median NDVI	572.2937	3.5	-0.004629
tagging site	574.3730	5.6	-0.0101
ordinal date + tagging site	576.2354	7.5	-0.01453
ordinal date * tagging site	578.6583	9.9	-0.01693

SUPPLEMENTARY TABLE 7 Candidate models set for the core areas and the respective predictor variables showing performance of the top model relative to others in the model set. The models are ordered from the lowest to the highest delta AIC value (dAIC, i.e., calculated difference between the AIC value of the observed model and the candidate model with the lowest AIC). The simbol '*' in the column "Model and predictor variables" indicates interaction between the two variables tested in respective model.

Model and predictor variables (50% kernel)	**AIC**	**dAIC**	**Adjusted R^2**
accumulated rainfall 6 months	567.9202	0.0	0.01699
season * tagging site	568.9034	1.0	0.03125
real coordinates median NDVI	569.0634	1.1	0.01139
season + tagging site	569.1104	1.2	0.0208
null	570.3730	2.5	
random coordinates median NDVI	571.0147	3.1	0.001743
accumulated rainfall 12 months	572.1871	4.3	-0.004096
tagging site	574.3730	6.5	-0.0101
ordinal date + tagging site	576.2865	8.4	-0.01479
ordinal date * tagging site	580.1843	12.3	-0.02468

SUPPLEMENTARY TABLE 8 Correlation matrix showing the Pearson's correlation coefficients (r) calculated for the numeric predictor variables: ordinal date of the respective fortnightly subset, median of the NDVI data associated with the real coordinates recorded for the macaws ("Real NDVI"), median of the NDVI data associated with the random coordinates ("Random NDVI"), accumulated rainfall (in millimeters) over the last six months ("Rainfall 6"), and accumulated rainfall (in millimeters) over the last twelve months ("Rainfall 12").

	Ordinal date	**Real NDVI**	**Random NDVI**	**Rainfall 6**	**Rainfall 12**
Ordinal date	1.0	-0.2	-0.3	-0.4	-0.2
Real NDVI	-0.2	1.0	0.9	0.7	0.6
Random NDVI	-0.3	0.9	1.0	0.7	0.7
Rainfall 6	-0.4	0.7	0.7	1.0	0.7
Rainfall 12	-0.2	0.6	0.7	0.7	1.0

SUPPLEMENTARY TABLE 9 Summary of the values of mean, median, standard deviation ("SD"), minimum ("Min.") and maximum ("Max.") of the distances (in meters) calculated from each input location ("Feeding" or "Resting") to the closest target site ("Roosting" or "Feeding").

Input locat.	**Target locat.**	**Mean (m)**	**Median (m)**	**SD (m)**	**Min. (m)**	**Max. (m)**
Feeding	Roosting	2,330.72	201.13	4,135.24	0.10	35,824.69
Resting	Roosting	2,754.65	361.52	4,450.96	0.13	35,765.94
Resting	Feeding	75.45	19.81	281.24	0.00	7,608.64

SUPPLEMENTARY TABLE 10 Summary of the number of GPS fixes (positions), for the identified locations ("Feeding", "Resting" and "Roosting"), where macaws stayed in a defined radius for a defined minimum duration (not moving faster than 1 m/s GPS ground speed), and the calculated values of minimum ("Min."), maximum ("Max."), mean and median of the time duration (i.e., time spent, in hours) inside the area of radius r (in meters).

		Number of positions	**Time duration (hours)**	**Radius (meters)**
Feeding	Min.	3	5	6
	Max.	121	11	999
	Mean	32	8	458
	Median	31	8	431
Resting	Min.	2	3	0.1
	Max.	121	10.5	49.9
	Mean	19.6	4.5	21
	Median	20	4.2	18.2
Roosting	Min.	2	9	1
	Max.	61	14	499
	Mean	11	12	178
	Median	10	12	160